DEGREE PROGRAMME IN WIRELESS COMMUNICATIONS ENGINEERING

MASTER'S THESIS

ACTIVE PHASED ARRAY TRANSCEIVER - AN OPERATIONAL COMPENSATION FOR A MULTIPLE PHASE SHIFTER SYSTEM

Author	Nédio Chrystian da Silva Neddef
Supervisor	Aarno Pärssinen
Second Examiner	Risto Vuohtoniemi
Technical Advisor	Marko Leinonen

April 2018

Da Silva Neddef N. C. (2018) Active Phased Array Transceiver - An Operational Compensation for a Multiple Phase Shifter System. University of Oulu, Degree Programme in Wireless Communications Engineering. Master's Thesis, 53 p.

ABSTRACT

The upcoming fifth-generation mobile technology relies on the implementation of beamforming techniques to fulfill the requirements proposed for the 2020 roll-out. One of the processes for stepping up this technique from the high-end applications to the telecommunication mass market is to be able to test, analyze and tune the product according to the specifications. After the manufacturing process, the phased antenna array, beamforming and beam-steering system must be tested against a prediction model, and corrected against deviations due to the uniqueness of the components, with the objective to conform the final product to be in accordance with specifications, while at low cost and time. The aim of this work is to propose and test different procedures for calibrating the phase component of an RF phased array transceiver with multiple phase-shifters. The different proposed procedures are compared in an over-the-air measurement through the performance when applying the beamforming and beam-steering techniques.

Keywords: active phased antenna array, beamforming, 5G, beam-steering, phase-shifters.

TABLE OF CONTENTS

FOREWORD

The present work concludes the Master Degree studies on Wireless Communications Engineering at University of Oulu, and was financed by the European Union Regional Project A71628 - Oulu radiotaajuustutkimuksen huipulle (RF excellence in Oulu) through the University of Oulu. The objective of the project is to maintain and improve Oulu's expertise as a RF technology developer and as an important contributor by conducting cutting-edge research, and training engineers to work in the area.

The Author would like to express his gratitude towards:

Marko Leinonen; Markku Jokinen; Nuutti Tervo; Olli-Erkki Kursu; Juha-Pekka Mäkelä; Risto Vuohtoniemi; Aarno Pärssinen; for the patience, guidance and support;

the 5GCHAMPION project for the possibility to use a radio transceiver prototype on the tests performed in this work;

the Center for Wireless Communications and the University of Oulu; for the learning opportunity and welcome during the exchange period (2014-15), and again, in the Master Degree studies (2017-18);

the Science Without Borders program, Brazilian Governmental institutions, CNPq and Capes, for the exchange opportunity (2014-2015);

and of course, my family.

Oulu, April, 10 2018

Nédio Chrystian da Silva Neddef

LIST OF ABBREVIATIONS AND SYMBOLS

3GPP	3rd Generation Partnership Project
5G	Fifth Generation of Mobile Telecommunications
AUT	Antenna Under Test
CLK	Clock Signal
DUT	Device Under Test
IF	Intermediate Frequency
IMT	International Mobile Telecommunication
ISM	Industrial, Scientific and Medical
ITU	International Telecommunication Union
LTE	Long Term Evolution
LTE-LAA	LTE- License Assisted Access
LTE-U	LTE-Unlicensed
RF	Radio Frequency
SGA	Standard Gain Antenna
SHF	Super High Frequency (3 GHz – 30 GHz)
SLL	Sidelobe Level
SNR	Signal-to-Noise Ratio
S-parameters	Scattering Parameters
UHF	Ultra High Frequency (300 MHz – 3 GHz)
VNA	Vector Network Analyzer
WRC	World Radiocommunication Conference

d	Distance
K	Total antenna element number
N	Number of branches of RF transceiver
r	Distance from the irradiating element
s	Number of phase-step of phase-shifter
λ	Wavelength
GHz	Gigahertz, 10^9 Hertz
MHz	Megahertz, 10^6 Hertz

mW	milliWatt, 10^{-3} Watt

1. INTRODUCTION

The ever-increasing demand for advances in communications systems is one of the main technology drivers pushing the knowledge boundaries. Not only has deep roots in the technology enhancement, absorbing, creating and sharing discoveries, but also plays an important role enabling new products and services. Few sectors have similar remarkable impact on human lives. Great cultural and social changes from the last century were hand-to-hand with communication systems, from radio and telephones, to television, satellites, internet, and cellphones.

On the verge of this technology boundary lie specifications and parameters that must be overcome as to enable a whole new spectrum of technologies, products, and services. At the present moment, the demands are for higher capacity, higher speeds, low latency, high mobility, among others. These parameters answer for better performance in existing situations, e.g. communications in high-speed trains; increasing demand, e.g. streaming services; enabling ongoing technology developments, e.g. driverless vehicles; and finally enabling technologies that are yet to come, making a new range products and services feasible, as cultivating a new fertile ground for ideas [1].

The main objective of the present work is a study of one of the most promising techniques to be deployed on the Fifth Generation of Mobile Telecommunications (5G), the antenna array beamforming. This work specifically aims to overcome difficulties, imperfections in the components and production, tuning the Radio Frequency (RF) transceiver final product to fit the minimum requirement for product delivery regarding the antenna array beamforming technique.

The main reason to perform such adjustment lie on the beginning of mass deployment of this technique, which is already used in high-end systems e.g. radars, military aircrafts, space industry, and defense industry; the implementation of the antenna array beamforming together with a Super High Frequency (SHF) transceiver, both new deployments to mass market, will challenge the companies at development and production stages [2, 3]. Similarly to other complex and niche technologies that debut on the mass market, the costs in the early stages will be high, there will be few suppliers and also few choices in the component level, even quality will be lower at this stage [4]. To partially mitigate these constraints, the ability to tune the final product to the minimum quality required for delivery can prove itself useful, regarding ramp ups, and lowering the production costs, only to mention a few purposes.

Therefore, this work is divided into the following chapters, which will be briefly described.

Chapter 2 explores some of the necessary concepts and technologies, the focus is on the phased antenna array and beamforming, concepts as 5G, SHF systems, and components as phase-shifters are also explained paving the base layer for the continuing of the work.

Chapter 3 presents a succinct literature review about testing RF systems, the focus is given towards the test environment for Over-the-Air (OTA) measurements, where, the basic parameter analysis of an antenna is presented alongside the different setups for measuring the antenna pattern depending on facilities available. The chapter continues with a review of some of the distortions, errors and other issues that can be found in the RF transceiver analysis.

In Chapter 4 various methodologies of the tests are presented, along with the underlying reasons. In this chapter, the constraints of the tests are commented and analyzed, further analysis is presented in detail in Chapter 5, which in line with Chapter 4, demonstrate the constraints of the procedures of the tests and results. The applicability of the tests and the solution regarding the tuning options are also discussed. Four tests are proposed, Test 1 is a full characterization of the phase difference using the vector network analyzer. Test 2 uses the spectrum analyzer and power measurement as a proxy to characterize the phase difference. Test 3 uses the method of Test 2, while it aims to characterize the phase differences across the different branches of the RF transceiver. Test 4 presents a variant of Test 1, regarding the length and accuracy trade-off. Finally, Test 5 applies the characterization of the phase differences and presents the results with the beamforming and beam-steering technique examples.

Chapter 6 presents the final remarks on the constraints and concerns of the techniques, applicability of the solutions, and points opportunities for future developments. A brief summary is presented in Chapter 7.

2. DEFINITIONS

Aiming to perform the tests that lead to the tuning of the antenna array beamforming technology, a few concepts and definitions are necessary. Beginning from the 5G technical requirements to the reason to use the antenna arrays. Other concepts such as the beamforming and phantom cells are clarified and examples are further given.

2.1. A New Paradigm: The Fifth Generation of Mobile Communications

Following the progress of the radio communication technologies and targeting the demand forecast for the next decade, the International Telecommunication Union (ITU) started from 2013 onwards studies related to the future of mobile telecommunications.

Some of the first results were presented at the recommendation ITU-R M.2083 International Mobile Telecommunication (IMT) Vision "Framework and overall objectives of the future development of IMT for 2020 and beyond", which addresses the forecast of the demand with a recommendation of capabilities to fulfil the expected scenarios for the future.

At the present date, the guidelines referring to the minimum requirements for the IMT-2020 are being discussed, and from the last round of discussions dating from February 2017, some of the technical requirements are [1]:

- *Minimum requirements for downlink peak data rate is 20Gbit/s*
- *The minimum requirements for uplink peak data rate is 10Gbit/s*
- *Target downlink "user experienced data rate" is 100Mbit/s*
- *Target uplink "user experienced data rate" is 50Mbit/s*
- *Downlink peak spectral efficiency is 30bit/s/Hz*
- *Uplink peak spectral efficiency is 15bit/s/Hz*
- *Minimum requirement for user plane latency for eMBB is 4ms*
- *Minimum requirement for user plane latency for URLLC is 1ms*
- *Minimum requirement for control plane latency is 20ms*
- *A lower control plane latency of around 10ms is encouraged though*
- *Minimum requirement for connection density is 1,000,000 devices per km^2*
- *Requirement for bandwidth is at least 100MHz*
- *Bandwidths up to 1GHz are required for higher frequencies (above 6GHz)*
- *Four classes of mobility are defined:*
  - *Stationary: 0km/h*
  - *Pedestrian: 0km/h to 10km/h*
  - *Vehicular: 10km/h to 120km/h*
  - *High speed vehicular: 120km/h to 500km/h*

An increase in the utilized bandwidth is an important component for achieving higher data rates. Bandwidth is scarce and any extra capacity needed for a 5G technology wouldn't be available adjacent to the frequencies used nowadays at Ultra High Frequency (UHF), since the spectra in the region is full of different wireless systems. Therefore, the solution has been to focus on the SHF range, which would also allow to overcome other difficulties regarding the aforementioned requirements, e.g. connection density and vehicular mobility.

2.2. Mobile Communications from 3 to 30 GHz

The Super High Frequency (SHF) names the 3 to 30 GHz frequency range, with wavelengths spanning from 10 to 1 cm, respectively.

The SHF inner frequency bands can be divided within its use. The lower SHF, 3 to 10 GHz, is used for aeronautical navigation, fixed-to-satellite (earth-space communications), fixed and mobile communications. Between 5 and 6 GHz, there are Wi-Fi channels at the Industrial, Scientific and Medical (ISM) band. Regarding the frequencies from 3 to 10 GHz, Long Term Evolution (LTE) bands 22 (3,4 – 3,6 GHz), 42 (3,4 – 3,6 GHz), and 43 (3,6 – 3,8 GHz) are being implemented at the moment. Also, the concept of LTE-Unlicensed (LTE-U), or LTE- License Assisted Access (LTE-LAA), has been introduced by the 3rd Generation Partnership Project (3GPP), which through carrier aggregation allows to increase the operational bandwidth using unlicensed spectra, focusing at the 5 GHz ISM band. The middle SHF, 10 to 20 GHz, deals mainly with satellite communications, fixed and mobile to satellite, earth and space research, using satellites. While the high SHF, 20 to 30 GHz is used mainly for fixed and satellite communications [5].

The technologies used in manufacturing the highly specialized solutions for the middle and high SHF frequency bands, and its lower quantity demands, makes these frequency bands a different market when comparing the needs of a massive deployment of mobile communications to point-to-point and satellite communications solutions. The initial difficulties and investment needed determine the high cost of implementation at the beginning of the deployment. Nevertheless, within time, research, and new entrant companies and technologies, it should push development and consequently drive the prices down, with further increases in quality and reliability. Therefore, not only the mass market for mobile communications will benefit from the new frequency bands, as will the other technologies that use these frequencies, e.g. fixed and satellite communications will experience positive spillovers.

The different aspects of the frequencies at the lower, middle and higher SHF allows the use of the Phantom Cell concept [6, 7], which gained ground and is expected to be deployed within the 5G technologies. In this concept, an area is supplied by a macro cell which could operate in the usual UHF, 300 MHz to 3 GHz, or lower SHF band, according to the network and coverage criteria, providing control plane features, call and mobility control. While within this macro cell, there will be a selected number of small cells which will operate in the middle and high SHF with higher bandwidths. These small cells would provide user plane connection features and would operate in the middle and high SHF with higher bandwidth, with the objective to comply with the 5G technical requirements providing high data rates, user coverage, user density capability, etc. [6, 7].

In Figure 1, a phantom cell case is exemplified with the characteristics aforementioned. In the example four small cell units are formed from massive-element antennas.

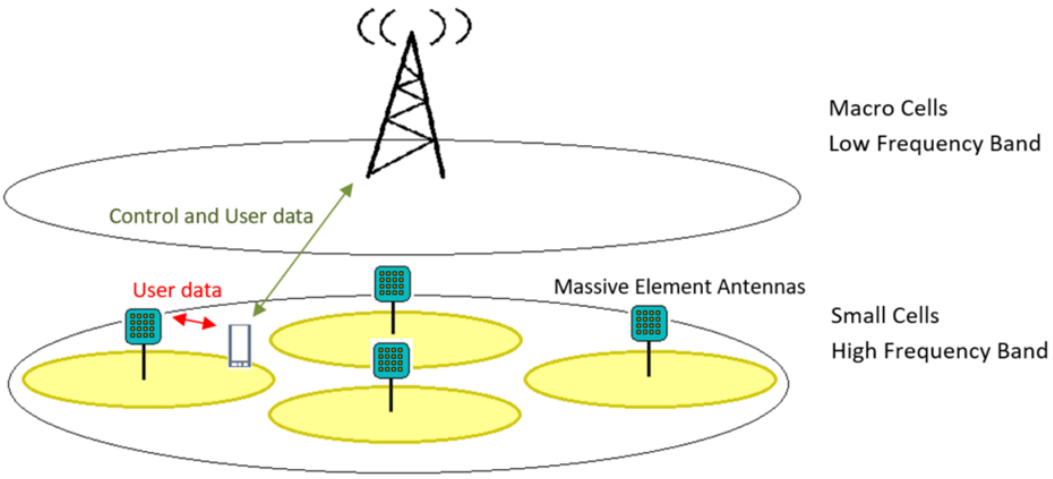

Figure 1. Phantom Cell concept.

An example for the usage of the Phantom Cell concept is the high mobility scenario regarding high speed trains, where one or more small cells could be deployed in the train, to concentrate traffic and reduce signaling.

The following concept, the phased antenna array, uses the wavelength properties of the SHF's for constructing a size-feasible array of antennas and further contribute to achieve the technical requirements for 5G.

2.3. Phased Antenna Array and Beamforming

A phased antenna array consists of two or more antenna elements (an antenna array), through which transmitted or received signals are, respectively, coherently divided or combined in order to enable the synthesis of a highly directional steerable beam [8].

Such method can be further used to overcome path loss and improve Signal-to-Noise Ratio (SNR) performance. Also, nullify interferers through the spatial division characteristics, minimizing contributions from noise and unwanted signals from directions different than desired. Using the aforementioned capabilities allows the possibility for multiuser MIMO, through the separation of the array in smaller cluster areas [9, 10, 11]. The characteristic of synthesizing a beam from a phased antenna array is named beamforming, and its steering ability is named beam-steering.

An example of an antenna array can be seen in Figure 2, a linear array antenna, where the K antenna elements at a distance d from each other, feed a summing network, in the example, a corporate feed type, using equal path lengths to the sink. While, in transmitter mode, the network would divide the signal to the K elements [12].

Besides the antenna itself, antenna arrays can be classified regarding the presence of amplifying components in its elements, an active array has for each antenna element an amplifying component, while, these are not present in the antenna elements of a passive array [8].

An example of a linear array with these components can be seen in Figure 3, where the symbols ∅ represent a phase-shifter component and ⊿ represent an attenuator component [13].

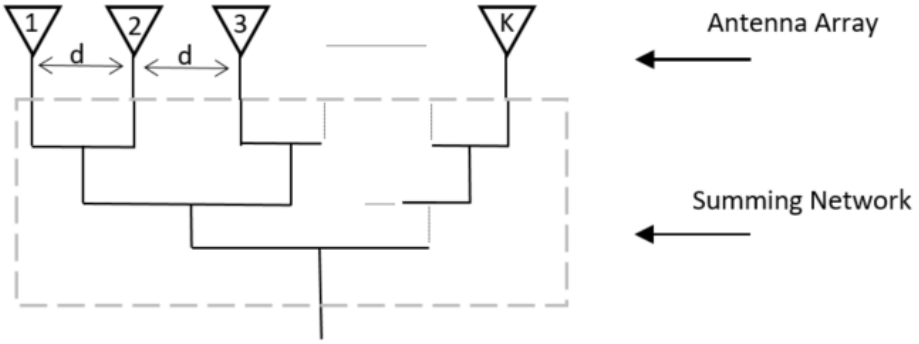

Figure 2. Linear array antenna and corporate feed summing network.

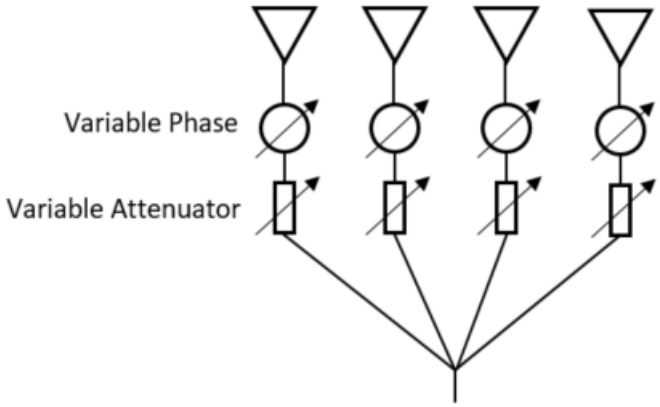

Figure 3. Linear array in receiver mode, with phase and amplitude control components.

At reception, the signal goes through the antenna elements, other components and summing network, through this process the signal at each branch is changed in phase and amplitude to be coherently added and to correspond to the desired reception pattern. While, at transmission, the process occurs from the distribution network and components to each branch and antenna element. The signal must be divided regarding the phase and amplitude characteristics of each branch and components, to produce a coherent transmission signal according to desired pattern.

To comply to this objective, different techniques can be used. In the digital beamforming, the RF signal can be sampled at each element and sent to a digital processor for complex weighting (amplitude and phase control) to construct the beam. In the analog beamforming, a change in phase can be an outcome from a change in frequency and/or time variables. Considering the time variable an interaction between distance and velocity, where the latter is derived from the permittivity and permeability of the medium. In the analog domain, a change in phase can be derived from the changes in the frequency of the signal; length, permittivity and permeability of the medium [12, 13].

For the purpose of communications, the frequency is a fixed parameter defined by the communication system and its frequency allocation. Therefore, it cannot be used for phase shifting. Permittivity changes can be accomplished with the use of specific materials, e.g. ferroelectric materials, in which the permittivity is a function of an applied electric field. Permeability is also material dependent, e.g. ferromagnetic materials, in which the permeability changes as a function of a change in an applied magnetic field [12].

Following the array and beamforming concepts, it is important to understand how the transmission pattern outcome is affected by the antenna array configuration and frequency, i.e. how behaves the beam and its parameters, shape, width and range [8]. To exemplify this interaction an interesting comparison was performed by [7], where three antenna array sizes were compared (20×20 cm; 40×40 cm and 80×80 cm) over three frequencies (3,5 GHz; 10 GHz and 20 GHz), results are summarized in Figure 4.

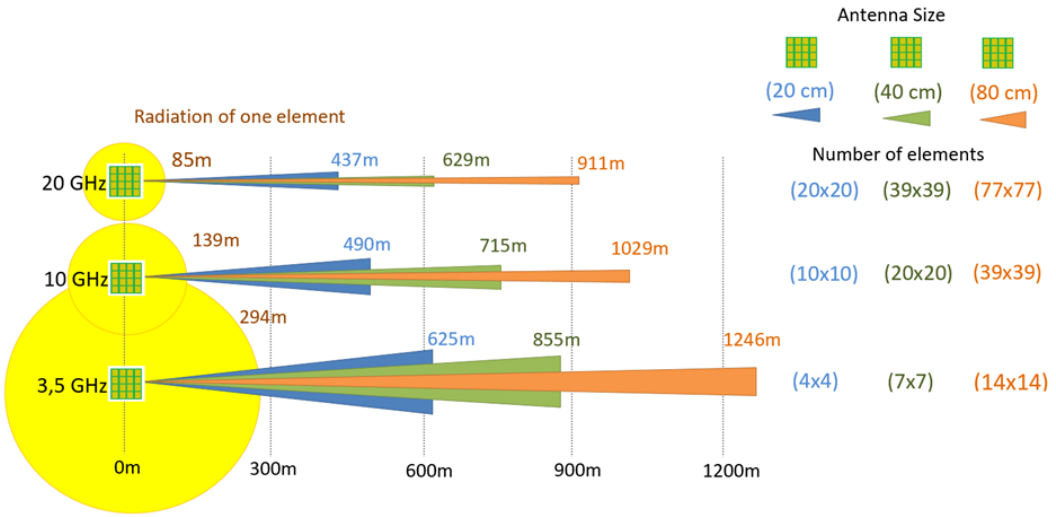

Figure 4. Comparison between, array sizes, antenna elements, frequencies, attenuation, and transmission pattern, according to [7].

The 3,5 GHz frequency was chosen regarding to the vicinity of 3GPP frequency bands for LTE, paired band 22 (3,41 – 3,49 GHz for uplink, 3,51 – 3,59 GHz for downlink) and unpaired bands 42 (3,4 – 3,6 GHz) and 43 (3,6 – 3,8 GHz). These frequencies have been partially identified for IMT at World Radiocommunication Conference (WRC)'07 (3,4 – 3,6 GHz) and identified globally for IMT at WRC'15 (3,3 – 3,7 GHz). Now defined as LTE bands 22, 42 and 43, they have been licensed in Europe for deployment of fixed, nomadic, and mobile networks; in Japan for terrestrial mobile services, and have also been licensed in countries in the American Continent [14].

The other two frequencies were chosen to be 10 and 20 GHz, as they represent a distinct separation while at the SHF band. Higher frequencies present higher attenuations, excluding at the moment, resonant frequencies depending on specific material, [7, 8, 12].

Given the combination of a fixed array size and different frequencies, while the distance between antenna elements in the array stays the same, half-wavelength,

the higher the frequency, more antenna elements can fit the array. Therefore, as an example, with the 20×20 cm array at 3,5 GHz, 16 antenna elements are present (4×4 matrix); while at 10 GHz, the array is formed by 100 elements (10×10 matrix), and at 20 GHz, 400 elements (20×20 matrix). The result of a higher number of antenna elements is a narrower beam and higher array gain to the direction of interest [7, 8, 12, 13].

Comparing the frequencies in the SHF with frequencies at UHF, where most of the mobile communications take place, the increasing interest on antenna arrays and beamforming technology can finally be explained. That is, not only by the gains the technology generates but also by the feasibility aspect. Systems at UHF, can be unfeasible in terms of cost, size, etc., given the wavelength and construction of the array. As an example, some specific frequencies and selected bands of LTE; in 700 MHz, the wavelength is approximately 43 cm and the half-wavelength 21,5 cm, which is the separation each antenna element would have in the previous example. In further examples the wavelengths and half-wavelengths are at 1 GHz (30 cm, 15 cm), at 1,5 GHz (20 cm, 10 cm), and at 2 GHz (15 cm, 7,5 cm), respectively. Comparing these values at 1,5 and 2 GHz, it can be demonstrated the unfeasibility regarding the required size of the array, with a 20×20 cm array only 4 elements (2×2) would fit, and therefore bigger arrays would be required to accommodate the same number of elements, and with lower frequencies that would only aggravate. Another effect also mentioned in [7], and shown in Figure 4 is the broadening of the beam generated by the array with lower frequencies. This, the aforementioned effects, along with other reasons, and the higher coverage of the single antenna element at these lower frequencies, contributed in a certain extent for the interest over the antenna arrays only for higher frequencies.

3. THE TEST ENVIRONMENT

In this chapter a succinct literature review about testing an RF system is presented. Since the outcome of a RF transceiver is analyzed, in general terms, through the antenna output, the focus is given towards the test environment for the OTA measurements. The basic parameter analysis of an antenna is presented, input impedance and radiation pattern parameters are analyzed. This chapter starts analyzing the aforementioned parameters together with different setups for measuring the antenna pattern depending on facilities available.

At the end of the chapter, the last section reviews some of the distortions, errors and other issues that can be found in the RF transceiver analysis, discusses the attention needed on correcting the errors with the objective to allow and improve the performance of the beamforming technique, therefore focusing on phase behavior.

3.1. RF system

Several tests must be made to certify the design of a system, RF components and systems are not different. A RF transceiver is a complex system of several components assembled into a structure, in which, manufacturing processes, faults, distortions, errors, and even, tolerance limits, affect the system outcomes [15].

The combination of individual components, manufacturing tolerances, and also, the resulting interaction of the components and structure within the assembled system, need to be tested. Not only, in the design and analysis stages to evaluate and certify products, but also different kinds of tests are mandatory during manufacturing with the objective to calibrate the final product [16].

The RF transceiver under analysis would require tests regarding its component features while working together, i.e. the overall test of the performance of the features of each component, e.g. gain from amplifiers, and spurious signals attenuation from filters.

For an overall analysis, measurements would include the input and output power, gain, gain compression, phase behavior, isolation, spurious events, harmonic behavior, stability, image rejection, noise, input and output impedance match, power consumption and so on [16]. Assuming the RF transceiver is functional, the main measurements for the matter of the present work have the objective to calibrate the transceiver towards the beamforming technique, by testing the phase behavior, output power, and gain [8, 12].

In the next section antenna parameters and test setups for measuring the RF transceiver are discussed.

3.2. Antenna Parameters

An antenna can be described using two parameters, input impedance and the radiation pattern [12].

The input impedance is derived from the Scattering Parameters (S-parameters) and can be obtained through self-coupling tests at the Vector Network Analyzer

(VNA). The VNA is a microwave receiver test system, which can determine complex ratios regarding the incident and reflected voltage wave amplitudes [12].

The Scattering matrix for a two-port system, according to [12], is given by Equations (1) and (2),

$$b_1 = S_{11}a_1 + S_{12}a_2 \quad (1)$$
$$b_2 = S_{21}a_1 + S_{22}a_2 \quad (2)$$

where b_1 and b_2 represents the complex voltage wave amplitude of the reflected wave at port 1, and 2, respectively. While, a_1 and a_2 represents the complex voltage wave amplitude of the incident wave at port 1 and 2, respectively. The coefficients of the system of equations form the Scattering matrix, and the coefficients are called Scattering Parameters. The S-parameter, S_{ij}, represents the coefficient of incidence of the wave from port i into port j, when $i = i$ or $j = j$, the incidence becomes a reflection.

To exemplify the incidence and reflection over a system, Figure 5 presents the excitation of one antenna in a two-antenna system and its effects,

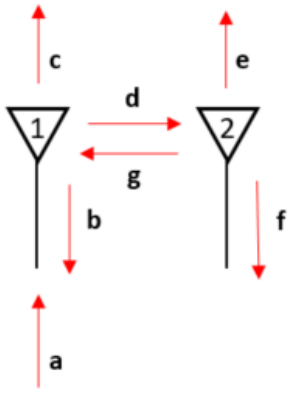

Figure 5. The effects of the excitation of one antenna element in a two-antenna system.

The antenna number 1 is excited by an incident wave (a), part of the incident wave is reflected (b), the other part is radiated (c, d). From the radiated wave, a part (d) will arrive at the antenna 2, where part of the energy will be reradiated (e, g), and part fed to the network (f); (g) is the reradiation arriving back at antenna 1 [12].

Given the behavior of high frequency systems the scattering matrix and the concept of incident, reflected and transmitted waves are more appropriate for analysis than the voltage, current, impedance and admittance analysis of parameters of low frequency systems; for further discussion [17].

3.3. Radiation Pattern Test Setup

Regarding the measurement of the antenna pattern, the specific behavior of the antenna towards the device under test (DUT), the facilities, and the equipment available, constrains what type and how the antenna and corresponding DUT can be tested.

During tests, non-desired effects must be avoided, or reduced, e.g. reflections. In order to do so, tests are performed in controlled environments such as the anechoic chamber, which is an environment where all the measurement range, i.e. floor, ceiling, walls and supports, are lined with radar absorbing materials consisting of titles made of carbon-impregnated foam, which are often shaped as pyramids [12].

Figure 6, demonstrates a test setup, where a Standard Gain Antenna (SGA) and an Antenna Under Test (AUT) are part of a test conducted in an anechoic chamber [12].

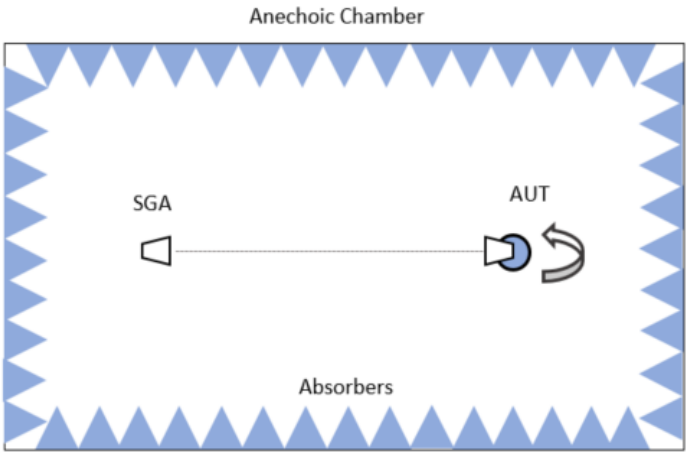

Figure 6. Example of test setup in an anechoic chamber.

The following relevant matter for the antenna pattern measurement is the distance range of the test, different techniques must be applied regarding the distance the antenna is positioned and its operational frequency. To retain a simple treatment of the matter, there are two main regions of analysis of an antenna according to its transmitted wave properties, the near-field and the far-field [13]. With r being the distance from the irradiating element, and λ the wavelength, a distance $r \ll \lambda$ characterizes the near-field, which by its properties, stores energy in its electric and magnetic fields similarly to a reactive device. While a distance $r \gg \lambda/2\pi$ characterizes the far-field, where the angular distribution around the antenna is independent of the distance [13].

The most common measurements are performed in the far-field region, and therefore, the anechoic chamber might impose a constraint on which types of antenna, and which frequencies can be tested.

Once the anechoic chamber is too small for intended tests i.e. when the wavefront deviates from the intended planar wavefront, a new setup can be arranged to conciliate the available space and the DUT to a far-field planar wavefront test. A planar wavefront can be synthetized over a Compact Antenna Test Range setup, which would generate a planar wavefront in a short range utilizing reflectors, an example setup is presented in Figure 7 [12].

Measurements can also be performed to evaluate the near-field, one possible setup configuration would be to sweep, scan and analyze a plane in the near-field. Figure 8, presents a planar near-field range setup, where a probe mounted in a planar

frame scans the AUT [12]. To obtain the radiation pattern, the near-field sampled data is Fourier-transformed, this technique works better for highly directive antennas.

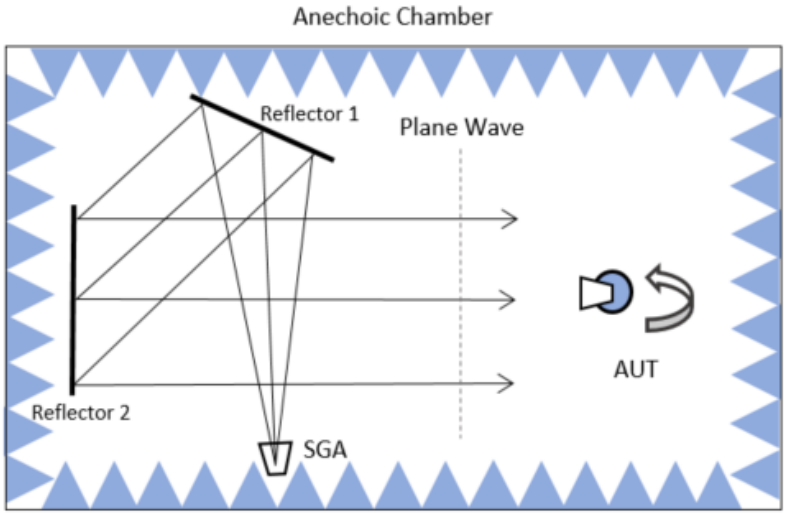

Figure 7. Example of a Compact Antenna Test Range test setup.

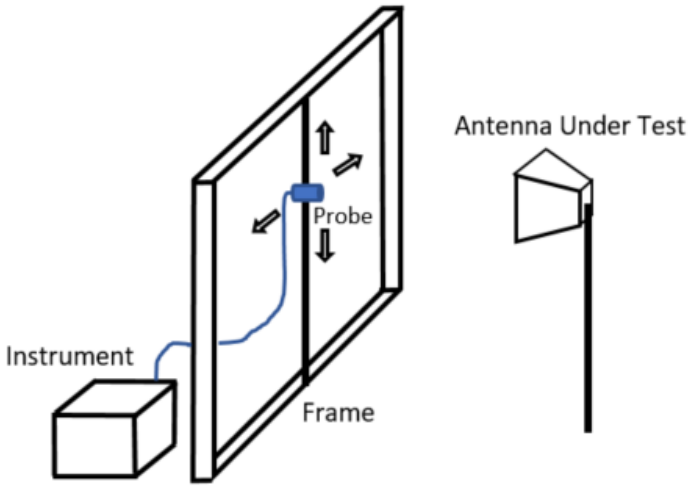

Figure 8. Example of planar near-field range setup.

Advancing towards the measurements of phased arrays, not only an array can be measured in full operation, but also by clusters or single elements. Assuming similar environment and effects for all the elements in the array, e.g. mutual coupling effects from surroundings, it would allow the radiation pattern from a single element of a large phased array antenna to be measured, while all other elements are terminated by matched loads. This would permit the approximate calculation of the phased array antenna performance given pattern multiplication, i.e. the single element measured multiplied by the array factor [12].

In the following section is presented a brief discussion on distortions and errors that arise during the measurements of an RF system.

3.4. Errors and Issues

When comparing the distinct branches of the array summing network, the differences between paths and individual components can result in a distortion of the expected signal within each branch, resulting in overall divergence. Such effect on the signal can be analyzed through a transfer function, illustrated by Figure 9.

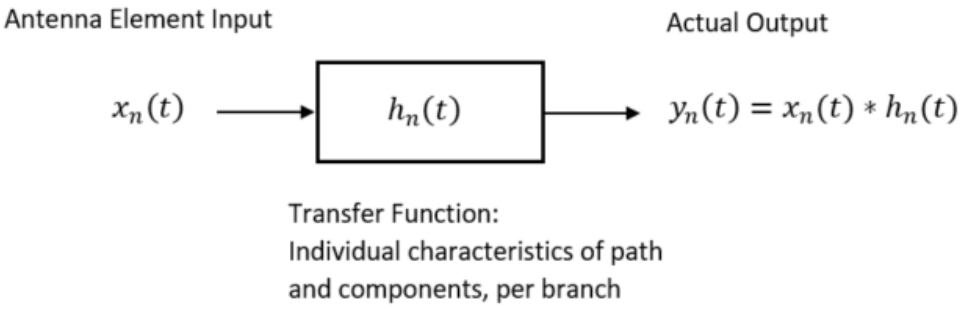

Figure 9. Transfer function diagram, effects of branch deviations.

Overall, there are two types of errors, systematic and random errors. The first type, which is composed of correlated and bias errors, is caused by a multitude of events, from manufacturing to environmental conditions. The designer objective is to remove all correlated errors, to be left with the uncorrelated residual, phase and amplitude errors, given by the manufacturing precision. The presence of distortions and errors, in amplitude and phase, lead to an increase in the level of sidelobes, the appearance and shift of grating lobes. The second type of error can be attributed to unquantifiable deviations, uncertainties of measurements, etc. Therefore, the treatment for this type of error is to perform a measurement calibration to account for, and minimize the test environment error; together with a proper statistical analysis to understand the sources of errors and quantify the amount of random errors [8, 18].

Specifically, the physical path and components are prone to deviations along the manufacturing tolerances, including dynamic errors caused by the environment where they are operated/tested. Those must be accounted, analyzed and calibrated within each branch of the array summing network and equalized within the network, [15].

The test itself is also a source of distortions which should be accounted and calibrated within the test. Test performance and results are prone to measurement errors from components, cables, adaptors, etc. Among the distortions are extra loss, impedance mismatch, loss of stability and so on [16].

Systematic errors can be characterized in three types, frequency response, mismatch and leakage. From the four types of transmission/reflection measurements included in the scattering matrix and S-parameters, input and output reflection, forward and reverse transmission, together form a twelve-error-parameter combination to be accounted and calibrated [16].

The idea behind the calibration process lies on applying a correction before starting receive/transmit the signal, which is called pre-distortion correction. Or to calculate and later apply the correction on the data, called post-distortion correction. Along these, the calibration process can be performed on-line or off-line, i.e. an on-line calibration would correct dynamic errors e.g. temperature shifts and component

ageing. While an off-line calibration, which could be a one-time calibration, would correct static errors, e.g. account for the manufacturability distortions. It is important to note that errors in the calibration process are also possible and would lead to further distortions in phase and amplitude. A calibration error that would wrongfully assert the element positions would also cause distortions in the reception/transmission direction of the array, and lead to wrong outputs [15].

The interaction between the antenna elements is also an issue. The electromagnetic coupling between the elements, i.e. mutual coupling, can result in a different behavior of gain and radiation pattern of the elements in the array, when compared with the single element. The shape and position of the elements in the array also will influence the behavior of the elements due to the different arrangement of elements in the vicinity [15]. In the case of mutual coupling the distortions would be accounted in the off-line calibration.

An antenna array performance is dependent on its elements and branch components. A fault in hardware can cause an element failure leading to diminishing performance due to increasing in beamwidth and sidelobe level, and even reducing the degree of freedom of the system. Further concerns are the need to recalculate the phasing of the elements, to avoid instabilities, appearance of unwanted grating lobes, and beam positioning errors [15].

As beam positioning is one of the main properties in the beam-steering technique and multiuser space division, an error in achieving the desired direction might cause the opposite of the desired effect, e.g. a wanted signal may enter a radiation pattern null. And instead of being transmitted/received is being treated as interference and cancelled [15].

Given the beamforming and beam positioning techniques and the need for precise phase control to enable those techniques, phase selection and precision are the cornerstone of the antenna array designed for these techniques. Errors in phase when not corrected or accounted in a calibration process lead the system to behave in an unexpected manner and therefore to fail according to operational specifications. Static phase errors typically occur due to imperfect phase-shifters and quantization errors. Along the phase errors, the calibration also must account for the frequency phase drift, which is the different propagation of the wave, and therefore, resulting phase observed within different frequencies. This phase drift is of special concern when designing a wideband system [8, 15, 18].

To exemplify the effects due to phase and amplitude errors in the level of the sidelobes a statistical method is presented by [8]. The author presents a phase and an amplitude error, which are described individually by a Gaussian probability density function, while the failed elements are randomly distributed. Continuing with a normalization regarding the peak of resulting pattern the author reaches the normalized sidelobe level, also called array average sidelobes or residual sidelobe level. The author performs an important comparison between the impact of phase and amplitude errors to the level of the average sidelobes. A proposed reduction in directivity given residual errors is also presented, in the authors derivation a reduction in directivity is not function of array size, but only, of error variance. Unless the array is considerably large, the effect of sidelobe distortion would be more severe than a directivity reduction [8].

The main source of expected phase error is due the manufacturability/cost trade-off of the phase-shifters. Although the desired phase-shifter would have a continuous function, this does not occur. The available phase-shifters will have

discrete values given by the bit discretization, e.g. a 3-bit phase-shifter will have 8 stages, i.e. the minimum precision is a 45° phase change, which will introduce highly correlated errors known as quantization errors. The results of the aforementioned errors are, lower performance, failure in achieving desired radiation pattern and beamforming, and also the appearance of sidelobes. Considering the phase- shifters further, there is still the manufacturing tolerance of the component, and this also adds to the output phase error [8].

The discretization of the phase-shifter will only allow a staircase approximation of the required continuous phase shift, this can be seen in Figure 10.

As an example, for the effects of phase quantization error, Figure 11 is presented. Phase-shifters with different bit quantization are compared and related to the number of antennas elements and the effect on the sidelobe level. Although this example is specific due to the hypotheses made, regarding the antenna and its transmission patterns, it provides an insight on the phase quantization errors on the array operation [8].

The quantization error periodicity of the phase, also adds to the sidelobe level problem, this is due to the correlation of the phase errors along the array. A series of methods to address the periodicity problem is briefly analyzed in [8], where the author summarizes some of the techniques that have as objective not the reduction of average error, but to diminish the periodicity of the quantization error, and therefore, affecting the correlation and reducing the peak sidelobes.

Following, in the next chapter tests are proposed to address the main concerns just discussed.

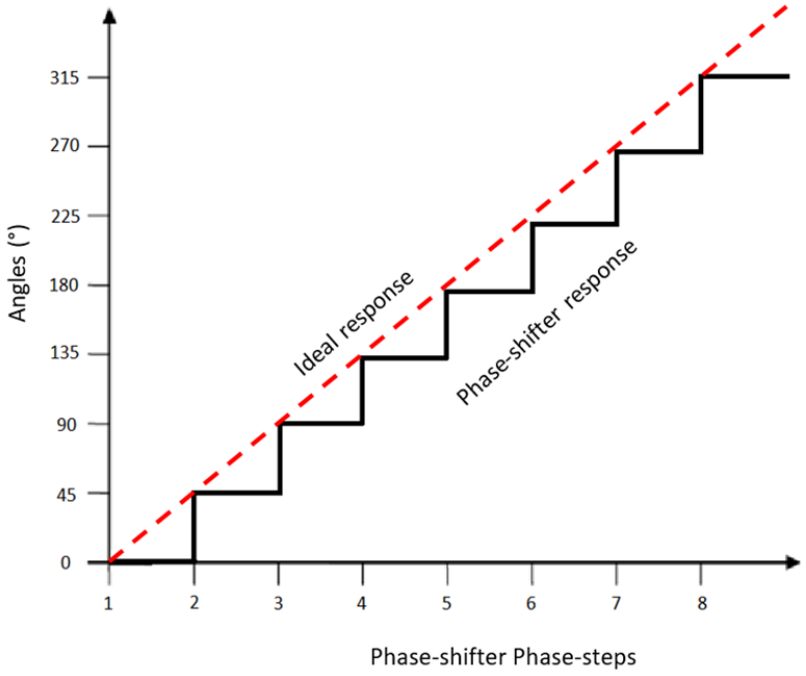

Figure 10. Phase quantization due to phase-shifter response.

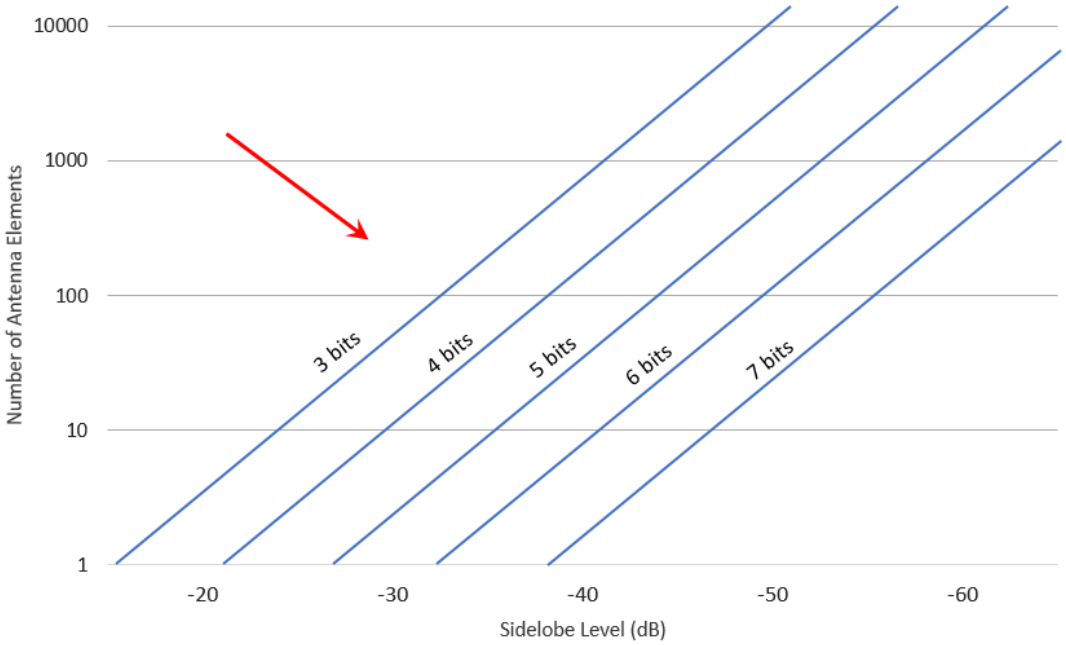

Figure 11. Number of antenna elements to attain a sidelobe level due to phase-bit quantization.

4. METHODOLOGY OF THE PROPOSED TESTS

Within the objective to calibrate the RF transceiver to allow a better performance of its output, it is important to comprehend and combine the system under test and the facilities. That is, input, desired outcome, tunable characteristics and equipment, software, location, etc. The aim of the present chapter is to propose a series of tests, combining the system under test and its specific configurations to the facilities. In order to analyze and finally propose a suitable method to calibrate the RF transceiver, in the next chapter.

The DUT used in this work is a RF transceiver, presented in Figure 12. It is an early prototype from the 5GCHAMPION Project [19, 20]. The device operates between 26 and 30 GHz and its final stages consist of a corporate feed network for a three level Wilkinson power divider, which creates eight individual branches. Each branch has a 5-bit digitally controlled phase-shifter. Besides that there are specific paths, for receiver mode there are low noise amplifiers, and for the transmission mode there are power amplifiers. This prototype can be connected to an array antenna also developed by the project, consisting of a 2×2 subarray antenna for each branch, forming a 2×16 planar array antenna; more details can be found at the project references.

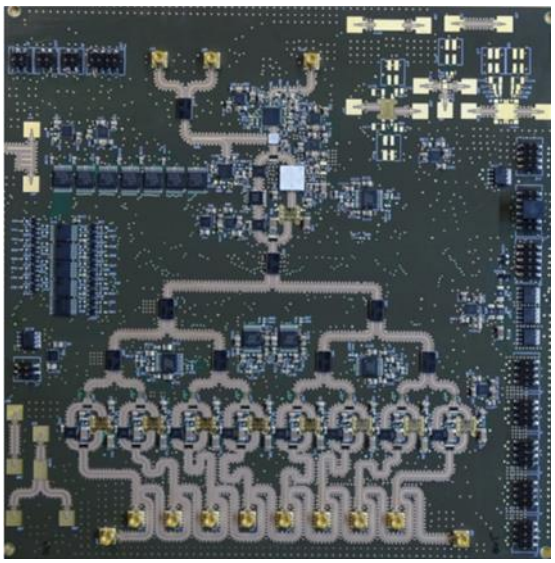

Figure 12. Device under test: RF transceiver.

Each following section of the present chapter proposes a different test to ascertain the characteristics of the output and feasibility of the test itself. Therefore, it does not only aim to calibrate the DUT but to determine the trade-offs of each test, e.g. accuracy vs. test time.

The tests are divided between conducted and OTA tests. From the conducted tests, the aim is to establish the relative phase output at different branches of the DUT, starting from the complex and resource consuming test using a VNA to perform a frequency conversion test over the spectra, to the simplest, power test using a spectrum analyzer.

Finally, the OTA test evaluates the success of the calibration regarding the radiation pattern, towards the beamforming and beam-steering techniques.

4.1. Test 1: Phase Difference Characterization

The main goal of the tests is to calibrate the phases of the DUT in the most accurate manner given constraints, e.g. time, relative error, expenses, etc., to obtain a set of relative phases.

Once this set of phases is established, the beamforming among other techniques can be applied. That allows the possibility to accomplish different results, e.g. reduction of sidelobes, construction of null areas, multiple beam formation, beam-steering, etc. As an example, given a wanted beam-steering direction, a constraint optimization from the set of available relative phase values can minimize the error and choose an optimum subset of phase-shifter phase-steps regarding the wanted direction.

The use of digital phase-shifters adds quantization issues, aforementioned, and usual component tolerance allows errors in the system. During the tests, it is expected to find errors apart from the 11,25° phase shift desired per step change along the 32 steps of the 5-bit phase-shifter, and further random errors.

The relative phase over every step of the phase-shifters, and also, the phase-shifter phase-step increment, can be measured through the use of the VNA, along with the differential and I/Q application software package.

For the Test 1, the RF transceiver operates in receive mode at 28 GHz. The test is done in conducted mode using a continuous wave signal and the output of the transceiver is an Intermediate Frequency (IF) at 4 GHz.

For this measurement, branch 1 is set as a reference, and the other seven branches (2-8) are measured against it, each set (branch 1 × branch N) is composed of 32×32 averaged trace measurements combining all the phase-shifter phase-steps. At each branch the traces record the parameters, power (dBm) and phase (°).

Given this specification, the test shows itself to be very long, therefore, for the purpose of the experiment only branches 1 (Reference) and 2 will be measured.

The instruments used are the VNA Keysight PNA-X N5247A, where VNA port 1 feeds the RF transceiver branch 1, VNA port 3 feeds branch 2, and the RF transceiver IF output feeds VNA port 2. A signal generator, Keysight PSG E8257C, feeds the required clock (CLK) to the operation of the DUT. A computer controls the operation of the instruments, VNA and signal generator and also, the DUT. This setup is presented in Figure 13. The results for this test are presented and analyzed in Chapter 5.1.

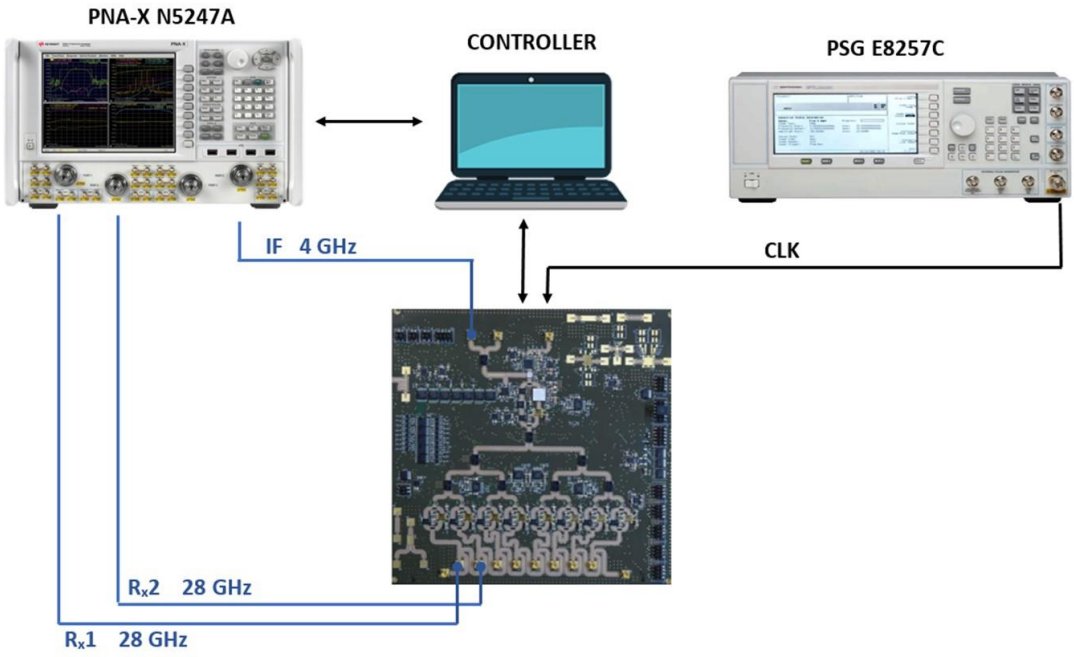

Figure 13. Test 1 setup.

4.2. Test 2: Phase Difference Test and Frequency Dependence – Using Power as a Proxy

The second test aims to discuss and tackle the time duration problem of the previous test. Together with it, the second purpose is to address the phase drift experienced when changing the frequency of the RF transceiver operation.

Although time duration decreases significantly in Test 2, there are considerable trade-offs. The first, the loss of degrees of freedom and consequently information, and in this case also, accuracy. The second is an increase in complexity of the analysis.

The main instrument used in this test is the spectrum analyzer, which focuses on the frequency domain analysis of signals. The test compares the output power of the RF transceiver along all the combinations of phase-shifters phase-steps. Using the signal properties, when equal signals are added with the same phase, they result in a signal with an increase of 3 dB in power, and when these signals are separated by 180° in phase, they result in a sharp drop in power, theoretically infinity, given the logarithmic properties.

The comparison can be performed in several ways, in resemblance with the Test 1, the maximum and minimum power value can be compared, and would have similar problems.

While in the case of Test 1, the accuracy could be better preserved given the superior level of information of the data set which allowed the use of the technique of finding the minimum and the phase distance regarding branches, it occurs differently in Test 2. In the latter the set of data is restrictive and the simply use of the minimum value of power to establish the phase values for all the table and assume that the theoretical phase-shifter phase-steps are 11,25° will propagate errors, given the phase-shifter phase-step increment errors, and deem the desired phase outcome unachievable.

To try to overcome these problems a different method of analysis can be used, the maximum and minimum power values are extracted, these power reference values can be taken regarding the whole table for branch 1 and branch N (32×32) or taken column-wise, i.e. for branch 1 step 1 the maximum and minimum values are taken from branch 2 steps 1 to 32. That is followed by branch 1 steps 1 to s, and later done for all other branches (3 to N) referencing to branch 1. After retrieving these values of power in dBm, they can be exponentialized to the scale of milliwatts (mW), which allows the construction of a reference table of phases regarding power levels. Both methods have pros and cons, and a set of hypotheses must be made for each of them.

When taking the maximum and minimum values from the 32×32 table, the main assumption is that there are no differences in power caused by the different paths that compose the phase-shifter component. And therefore all the signals combinations at the relevant phases have the same output power. This is a very strong assumption, and it will lead to severe errors depending on the branch-step chosen, empirically the different combinations of the two measured branches will have very different power levels for maximum and minimum points.

The second method, in which the reference is in a column or row-wise manner, assumes that regarding a reference branch and a phase-step, the full set of phase-step changes (1-32) of the second branch always has a value which makes the comparing branch phases very close to be similar or completely different, i.e. close to maximum and minimum. These values would then be established as 0° and 180°, respectively. Clearly, this method adds a systematic error due to the difference between the real relative phase at that combination of branch-step and the reference values set as 0° and 180°. This difference would also add to all the phase values column or row-wise while setting a phase-power table, due to the error in the reference values.

The spectrum analyzer power test assumes an accuracy-error trade-off against the time lenght of Test 1. Even with considerably more averaging samples, the spectrum analyzer power test is faster than the Test 1, made using the VNA.

Test 2 setup is presented in Figure 14. A signal generator (PSG E8267D) generates signals from 26 to 29 GHz of frequency, these signals go through a power divider and feed branches 1 and 2 of the RF transceiver. The RF transceiver is also fed with a clock signal (PSG E8257C). An IF signal is the output from the RF transceiver, and it feeds the spectrum analyzer (UXA N9040B).

Differently from Test 1 when the calibration of the support equipment, cables, and connectors was done by the routines of the VNA, in the present test the cables and power divider must be studied. The results acquired must be used to correct the error added by these components. To perform this correction a small test on the VNA is necessary to analyze the S-parameters of the cables and power divider, with the objective to gather the phase difference added between the power divider outputs and the RF transceiver.

Another simple test is needed to determine the direction of the phase change given a phase-shifter phase-step change at the branches. As an example, given the power at the maximum value and phase difference equal to 0°, any drop in power means that the phase difference is increasing. Although the direction in which the phase moved is not clearly seen from the power value, e.g., a change of 10° from the maximum would lead to 10° or -10°.

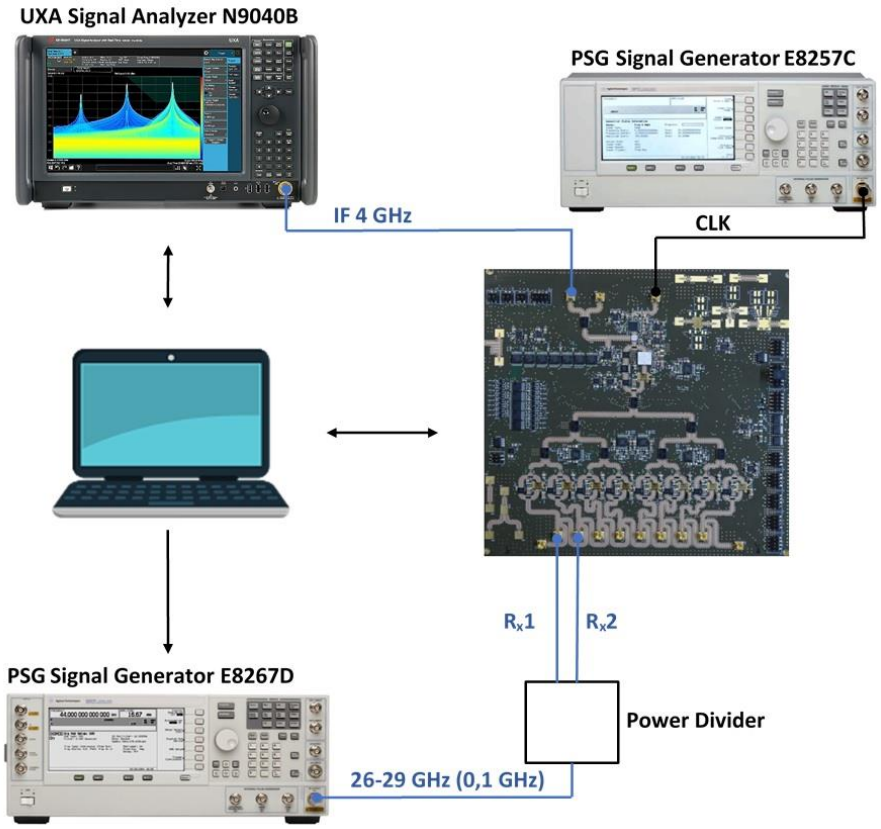

Figure 14. Test 2 setup.

The second aim is to exemplify the use of the method developed in this section with the important matter of the phase drift along the RF transceiver frequencies in operation. Different frequencies have different wavelengths, and therefore, while travelling the same media, the phase at the output will be different due to the phase rotation. For a phased array and given a set of phases for a desired beam direction this would lead to an offset from the desired angle of the beam, also known as beam squint. This factor impacts the limit bandwidth of the phased array system. As an example regarding the wavelengths, at 28 GHz the wavelength is 1,071 cm, and when dealing with small wavelengths and similar high frequencies any small variations can already cause bigger variations on the phase result. The difference between 28 and 28,1 GHz would produce an extra wavelength, a full phase rotation, in approximately 2,8 m. Results and further test explanation are presented in Chapter 5.2.

4.3. Test 3: Phase Difference across the RF Transceiver Branches – Using Power as a Proxy

The third test follows the steps from Test 2, using the power measurements of the spectrum analyzer as a proxy for constructing the phase characterization.

Test 3 uses the same method described in Test 2, but the measurements are done across the different branches of the RF transceiver. Seven measurements are done comparing the branch 1 (reference) with branches 2 to 8, the setup is similar to Test 2, except that the second output from the power divider feeds one branch at a time.

The setup is presented in Figure 15. A signal generator (PSG E8267D) generates a 28 GHz signal, which goes through a power divider and feeds branch 1 and branch N (2 to 8) of the RF transceiver, one at a time. A clock signal (PSG E8257C) is fed to the RF transceiver. As the output of the RF transceiver, the IF signal at 4 GHz, feeds the spectrum analyzer (UXA N9040B).

The goal behind the characterization of the phase difference across the different branches of the RF transceiver is to allow the construction of a map of all the relative phases. The map of relative phases would permit the selection and optimization of the subsets of the phases required for the beamforming and beam-steering technologies.

The results are presented in Chapter 5.3.

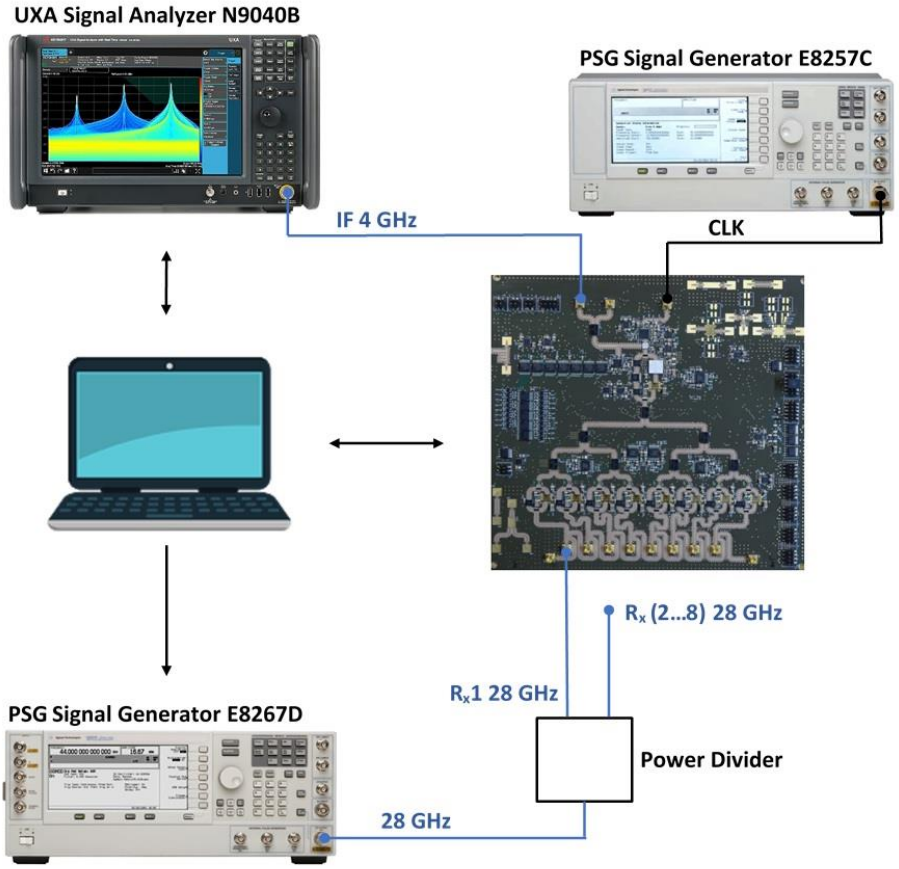

Figure 15. Test 3 setup.

4.4. Test 4: Phase Difference across the RF Transceiver Branches – A variant of Test 1

Within the need of a more precise test, given the length of Test 1, and to obtain a second feasible method to compare to the method of Tests 2 and 3, a compromise could be made in the method of Test 1, which would allow a shorter length variant.

The idea behind this variant is to decline the degree of freedom given by the phase-shifter phase-steps of the reference branch (branch 1) and doing so the number

of data gathered would reduce drastically. The measurement can be performed within one or few phase-steps of branch 1 and all the phase-steps of the other branches (2 to 8).

The problem is clear, the reduced degree of freedom leaves a reduced margin of tolerance regarding any defects on the reference branch phase-shifter component, and in the case the chosen phase-step is defective this might not be noticed. Other problem derived from the method is the non-optimality of the result. The phase-step chosen at the reference branch very likely will not be the optimum regarding the relative phase accuracy to a certain required phase, and therefore, will have an impact on the desired outcome.

The test setup is the same as Test 1 with one difference, all other branches are fed instead of only branch 2, and the reference. The Keysight PNA-X N5247A, VNA port 1 feeds the RF transceiver branch 1, VNA port 3 feeds branches 2 to N, the RF transceiver IF output, 4 GHz, feeds the VNA port 2. A signal generator, Keysight PSG E8257C, feeds the required clock (CLK) to the operation of the DUT, a further computer controls the operation of the instruments, VNA, signal generator, and the DUT. This setup is presented in Figure 16. The results are presented in Chapter 5.4.

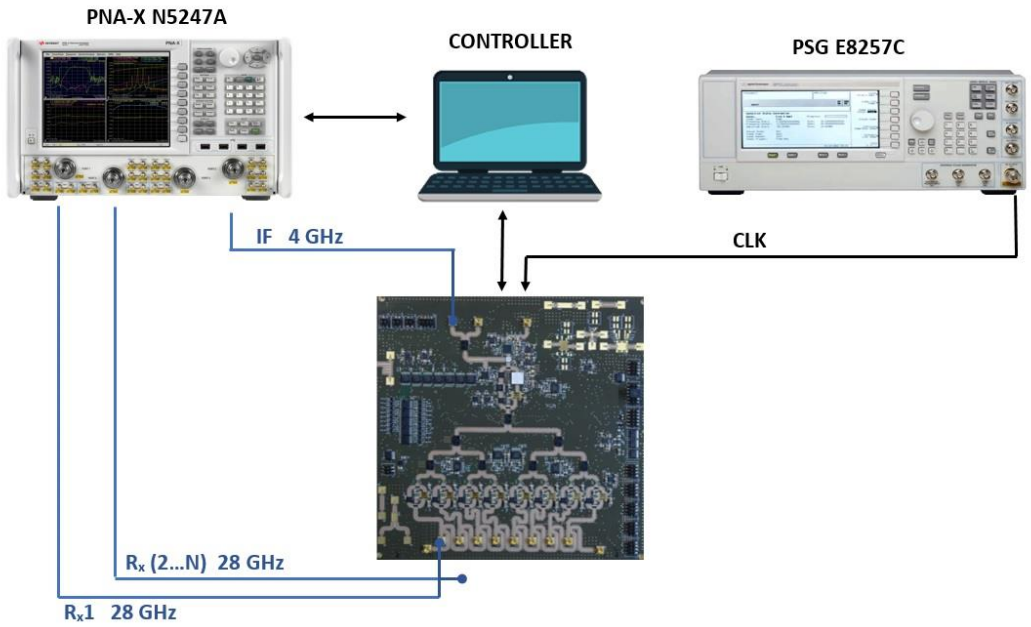

Figure 16. Test 4 setup.

4.5. Test 5: Over-the-Air demonstration - Applying the phase calibration for Beamforming and Beam-steering techniques

The last test aims to verify the methods of the phase calibration developed in the previous sections of this chapter, performing an OTA measurement.

The proposed test to validate the phase calibration is to combine coherently the phase of the outputs of the RF transceiver to perform the beamforming and beam-steering.

To do so, a setup is arranged in the anechoic chamber. The test consists of a far-field radiation pattern measurement (power over direction) gathered over 180°. A rotating table setup composed by a pedestal and a controllable step-motor turns the RF transceiver with an antenna array patch attached to a set of desired angles. The antenna array is positioned two meters from a standard gain antenna, the operation occurs in the far-field. In this setup the instruments can read the transmitted power from the standard gain antenna to the RF transceiver. The setup is presented in Figure 17.

The setup uses a signal generator (PSG E8267D) to generate a 28 GHz signal, which feeds a standard gain antenna (horn antenna) that transmits the signal to the patch antenna. The patch antenna is composed of 16 subarrays of 2×2 elements, each subarray can be connected to an active branch. It is composed of 2 columns of 8 subarrays, one of the columns is connected to the 8 branches of the RF transceiver, while the subarrays of the second column are terminated with 50 ohms. The RF transceiver receives the clock signal from a signal generator (PSG E8257C) and sends the output IF, at 4 GHz, to the spectrum analyzer (UXA N9040B). A computer controls the instruments, the RF transceiver and the rotating table. Results are presented and discussed in Chapter 5.5.

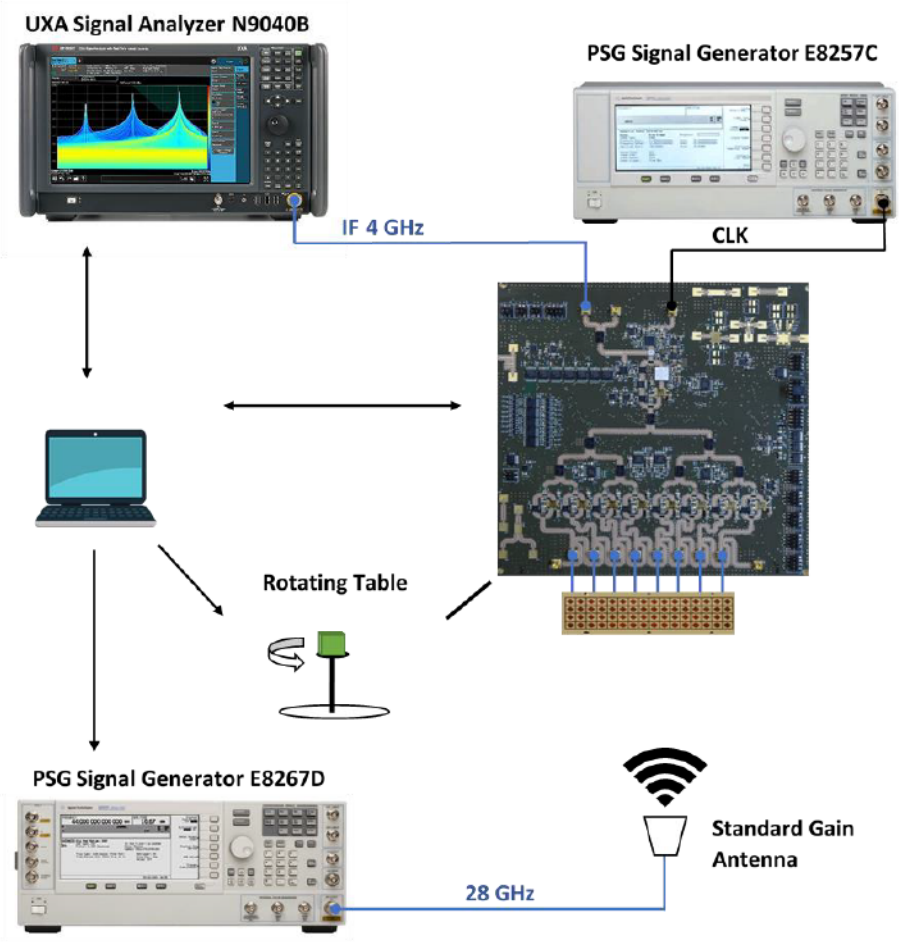

Figure 17. Test 5 setup.

5. TEST RESULTS

In this chapter the results of the tests described in Chapter 4 are presented and analyzed. Further explanation is given on the details and reasons behind each of the tests.

Manipulating the data retrieved from the measurements up to the analysis of the data presented in this chapter might not be a straightforward process. The process is explained, and at certain points detailed to allow the reproduction of the procedures used.

Sections 5.1 and 5.2 define two different measurement approaches to obtain the data on the phase relationship over the different branches of the RF transceiver. Sections 5.3 and 5.4 venture further on the previous approaches and define two simple and comparable calibration procedures, which are tested and compared against each other in Section 5.5, through a radiation pattern measurement.

5.1. Test 1: Phase Difference Characterization

The objective of the Test 1 is to obtain the relative phases given the phase-shifter phase-steps and errors, due component tolerance, distortions, system integration, and so on. In a theoretical construction, a change in the phase-shifter phase-step would cause a 11,25° change in the phase of the signal. This event is highly unlikely with high precision. Therefore, during this section a complex and time-consuming test that gives accurate results will be analyzed.

The system was calibrated and operated following [16]. The test comprises of constructing a trace, power (dBm) × phase (°), where branch 1 is used as reference, and each of branch 1 phase-shifter phase-steps (32 in total for each phase-shifter) are compared with the phase-shifter phase-steps of branch 2. At each combination (32 × 32), the trace is constructed sweeping the signal phase of branch 2, from 0° to 360°.

Using the signal properties, where equal signals added with the same phase result in a signal with an increase of 3 dBm in power. And these same signals when separated by 180° in phase are added, result in a sharp drop in power, theoretically resulting to zero power. This would result in a trace containing a maximum and a minimum power and phase values. The result of the analysis of the trace gives the phase distance between branch 2 signal phase and the points of maximum and minimum.

Knowing the phase difference between branch 2 signal phase and the point of maximum would give the distance in phase regarding branch 1 signal, and when compared with the point of minimum, it would give the distance in phase regarding 180° from branch 1. Since the point of minimum is sharper, and consequently, more accurate, that is the retained value.

This is not a straightforward process, and the collected data must be manipulated before the final result of phase difference between branches and phase-shifter phase-steps.

Overall, the test comprises of 1024 averaged traces, and last 11 hours and 30 minutes, if all branches were to be tested it would result in approximately 80 hours of test time. Since the test was just made at 28 GHz, the increase in the test frequency range would also increase the measurement length. A test made for every 100 MHz in

the RF transceiver operation range, would require 31 tests of approximately 80 hours each, resulting in approximately 2480 hours or 103 days, of course there is a major opportunity for optimization in the initial test but these values present the scale of the challenge.

The phase distance between branch 1 and branch 2, is presented in Table 1. The table has been normalized to present only positive phase values.

The colors represent:

- Orange: from 350° to 10°;
- Yellow: from 330° to 350°, and from 10° to 30°;
- Blue: from 270° to 330°, and from 30° to 90°.

The quantization effect is easily seen with the help of the color scheme, with the orange values representing the phase distance of the branches at maximum 10° from each other, the yellow values at maximum 30° and blue values at maximum 90°.

The quantization effect can also be seen in Figure 18, where two phase-steps from branch 1 were chosen to exemplify the phase difference. The ideal value of phase increment, 11,25°, is compared which phase-steps 1 and 32. Apart from the big change caused by the scale in degrees from 360° to 0°, it can be seen the stair shape caused by the quantization of the 5-bit approximation, plus extra deviations.

Being a detailed test, it allows a higher number of comparisons and extra information can be taken regarding the phase-shifters and its behavior. To understand exactly the impact of a phase-step change and its associated errors, the values of Table 1 are compared in a differential manner within a single branch. For each phase-step change in branch 1 there are 32 data observations at the different branch 2 phase-steps, allowing an analysis of the distribution of the results. Table 2 presents the data referring to minimum, maximum, average, and the standard deviation when assuming a normal distribution regarding the phase increment given phase-step change for branch 1. The normal distribution is used since it is the standard and there is no reason to believe that the systematic error distribution of the phase-shifter has any other behavior.

As an example, Δ32-1 can be read as a change from branch 1 step 32 to step 1, it has 32 values in accordance to in which phase-step was branch 2.

It can be seen from the standard deviation analysis that Δ32-1 and Δ31-32, detach from the other values. A deeper analysis of Table 1 and following the average and standard deviation gathered in Table 2, it can be seen that all branch 1 phase-step 32 values are the only ones from the table 1 to lie over two standard deviations of the normal distribution, clearly being outliers, therefore this specific phase-step might be considered presenting a fault. That is also corroborated by the Figure 18, where branch 1 phase-step 32 presents a non-expected, wave-like behavior.

The average phase-shift in branch 1 is illustrated in Figure 19. The increment at Δ31-32 was expected to be further from the mean, the graph also shows that at Δ15-16, the minimum and maximum increments are detached from the other values, possibly indicating a faulty phase-step.

The discussed errors might have been due to manufacturing, assembly of component or any kind of distortion, in the further analysis of branch 2 the data referring branch 1 Δ31-32 has been excluded.

Table 1. Test 1, phase difference (°) between branch 1 and branch 2

Branch 1 (step)		1	2	3	4	5	6	7	8	9	10	11	12	13	14	15	16	17	18	19	20	21	22	23	24	25	26	27	28	29	30	31	32
Branch 2	1	331,0	316,5	308,0	295,5	288,0	273,0	266,0	254,0	248,5	232,5	225,0	213,5	205,0	195,5	186,0	161,5	154,0	139,5	132,0	118,0	112,0	97,5	90,5	83,5	75,5	59,5	53,5	39,0	31,0	17,5	11,0	350,0
(step)	2	340,5	326,0	318,5	304,5	297,5	280,5	274,5	262,0	256,5	240,5	233,5	222,0	214,0	203,5	193,0	169,5	162,0	146,0	141,0	127,5	121,0	107,5	97,5	91,5	83,5	68,0	61,0	47,5	41,5	26,0	19,0	350,0
	3	355,0	341,0	333,0	318,5	311,0	294,5	288,5	278,0	271,5	254,5	248,0	235,5	228,5	216,5	208,5	183,0	176,5	162,0	154,5	142,5	135,5	121,5	114,0	106,5	99,0	84,0	75,5	63,0	56,0	41,0	34,0	13,0
	4	4,5	349,0	342,0	327,0	320,0	303,5	297,5	286,5	280,5	264,0	256,5	244,0	238,0	224,5	218,0	193,0	183,5	171,0	162,0	151,5	143,0	130,5	122,0	114,5	108,0	92,0	84,0	70,5	63,0	50,0	42,5	11,5
	5	15,5	1,5	353,5	338,0	332,5	316,5	309,0	299,0	291,0	276,0	267,5	255,5	249,0	236,5	227,5	203,5	197,5	182,0	175,0	163,0	155,0	141,0	134,5	126,0	120,0	103,5	97,5	83,5	75,5	62,5	54,5	32,0
	6	23,0	9,5	1,0	345,5	340,0	323,0	319,0	305,5	300,5	284,0	275,5	264,5	257,0	244,5	235,5	210,0	203,5	189,5	182,5	169,5	164,0	148,0	141,0	133,0	126,0	110,0	103,5	92,0	84,0	71,0	61,5	33,0
	7	40,0	25,0	16,5	2,0	356,5	339,5	333,5	321,5	315,0	298,5	293,0	278,5	271,5	260,0	253,5	226,5	219,0	204,0	197,5	185,5	178,0	164,0	157,0	148,5	143,0	126,5	120,0	107,5	100,0	85,0	77,0	56,5
	8	48,0	32,5	24,5	11,0	5,0	348,0	341,0	329,5	323,0	306,5	301,0	286,5	280,5	268,0	260,0	233,5	227,5	213,5	205,0	191,0	185,5	172,5	163,5	156,5	151,0	134,0	126,5	114,0	107,0	92,0	84,5	56,5
	9	57,0	42,5	35,5	20,0	13,5	358,0	350,5	338,5	332,5	315,0	309,0	297,0	291,0	278,0	269,0	245,0	237,0	222,5	214,5	203,0	196,0	182,0	175,0	166,5	159,5	143,5	136,5	124,0	117,0	102,0	94,0	72,0
	10	63,0	48,5	41,5	26,5	19,5	4,5	357,0	345,5	340,5	323,5	317,0	303,0	297,5	285,5	276,5	249,5	242,0	229,0	221,0	208,0	202,5	187,5	180,0	172,5	166,5	151,0	144,0	130,5	123,5	109,0	101,0	72,5
	11	82,0	67,0	59,0	44,5	37,5	21,0	14,5	2,5	356,5	340,0	334,0	321,0	314,0	302,0	292,5	266,0	260,0	245,0	238,5	224,0	217,5	204,5	197,5	188,5	182,5	168,5	160,0	148,5	140,0	126,5	117,5	98,0
	12	90,0	74,0	66,0	52,0	46,0	29,0	22,0	11,0	5,0	347,0	341,0	328,5	322,5	308,5	301,0	273,5	266,5	253,0	244,5	233,5	226,0	212,5	204,0	197,0	190,0	174,0	167,5	154,0	146,5	133,5	124,5	98,5
	13	101,5	86,5	77,5	64,5	57,0	42,0	33,5	22,5	18,0	359,5	353,5	342,0	332,5	321,0	313,0	285,0	278,0	265,5	257,0	244,5	237,0	223,0	216,5	208,0	204,0	186,5	179,5	166,0	161,0	145,5	137,5	119,5
	14	110,5	95,5	87,0	73,5	65,0	49,5	42,5	31,0	24,5	8,5	2,0	349,0	343,0	329,5	321,0	294,0	286,5	273,5	266,5	252,0	246,0	232,0	225,0	217,0	209,5	194,5	187,0	174,0	168,0	153,0	145,0	118,5
	15	123,0	108,0	100,5	86,0	79,0	64,0	56,5	45,0	37,5	21,0	17,0	2,0	355,0	343,5	334,0	308,5	300,0	286,0	278,0	265,0	259,0	245,5	237,5	229,5	223,5	208,0	200,5	187,0	180,5	166,0	158,5	141,0
	16	132,5	117,5	109,5	97,0	88,5	72,5	65,5	55,0	48,5	33,0	25,5	11,5	5,0	352,0	345,0	316,5	310,5	295,5	288,0	276,0	270,0	253,5	247,0	238,5	233,5	216,0	210,0	196,0	189,5	175,5	167,5	141,0
	17	157,0	141,5	134,0	119,0	112,5	94,5	87,5	76,5	71,0	54,5	47,0	34,0	26,5	14,0	7,5	338,0	332,0	318,5	311,0	297,5	291,5	278,0	269,0	262,0	257,0	240,0	232,5	219,5	213,0	198,0	191,5	172,5
	18	164,5	149,0	140,5	127,0	121,5	104,0	96,5	85,0	80,0	62,5	55,5	42,5	35,5	24,0	15,0	347,0	341,0	327,0	319,0	306,0	301,5	286,5	278,5	269,0	263,0	248,0	240,0	228,0	220,0	206,5	198,5	173,5
	19	179,5	164,0	156,0	142,5	133,5	118,0	111,0	100,0	94,5	76,5	71,0	57,0	51,0	37,5	30,0	3,5	354,0	341,5	335,0	321,5	315,5	300,5	293,0	284,5	280,0	262,0	254,0	242,0	235,5	221,5	213,0	196,0
	20	187,0	172,0	163,5	151,0	144,0	126,0	119,0	109,0	103,5	86,5	80,0	66,0	58,0	47,5	38,5	11,0	4,5	351,0	344,0	331,0	323,0	310,0	301,5	294,0	286,5	270,0	264,0	249,5	244,5	229,0	221,0	196,0
	21	200,5	184,0	176,0	163,0	156,0	138,0	132,0	120,0	114,0	98,0	91,5	79,0	71,5	60,0	51,0	23,5	16,5	1,5	356,0	343,0	335,5	322,5	313,5	305,5	301,5	284,5	276,0	264,0	255,0	240,5	233,5	216,5
	22	208,5	192,0	183,5	170,0	164,0	147,0	139,5	129,5	123,5	105,0	99,0	87,0	80,0	68,0	59,0	31,5	25,5	11,0	3,0	351,0	344,5	330,5	325,0	315,0	308,0	291,0	283,0	271,0	265,0	250,0	242,5	216,5
	23	222,5	206,5	198,5	185,5	178,0	162,0	154,5	144,0	138,0	120,5	114,0	102,0	95,0	80,5	72,0	46,5	39,5	25,0	19,0	6,5	0,0	345,0	336,0	329,0	321,5	307,0	298,0	286,5	280,0	264,0	257,5	238,5
	24	230,5	215,5	206,5	192,0	185,5	169,5	163,0	151,0	146,0	128,5	122,0	110,0	103,5	91,5	82,5	55,0	48,0	35,0	27,5	14,5	8,5	354,0	347,0	338,0	331,0	315,5	308,5	294,0	288,0	273,5	266,5	239,0
	25	239,5	224,5	214,0	200,5	193,5	177,5	172,0	161,0	155,0	137,5	130,0	117,0	110,5	98,0	90,5	63,0	55,5	42,5	34,5	22,5	16,5	1,5	354,0	346,0	340,0	323,5	316,0	303,5	296,5	282,0	273,0	253,5
	26	246,0	230,5	221,5	208,5	201,5	184,0	178,0	168,0	161,0	144,0	138,5	126,0	118,0	106,0	96,5	70,0	63,0	50,0	42,5	30,0	22,0	8,5	1,0	352,5	345,5	330,5	324,0	310,0	303,5	289,0	281,0	252,5
	27	262,5	246,5	238,5	224,5	217,5	200,5	194,5	182,5	178,0	160,5	154,0	141,0	134,5	122,5	113,5	88,5	80,0	66,5	58,5	46,0	40,0	25,5	17,5	9,5	3,5	345,5	340,0	326,5	321,0	304,5	297,5	276,0
	28	268,5	253,5	245,0	231,0	223,5	208,5	201,0	190,5	184,0	167,0	160,5	147,5	142,0	129,5	121,5	94,5	88,5	74,5	66,5	54,5	48,5	33,5	27,5	17,0	11,0	354,5	348,0	334,5	328,5	313,5	305,0	277,5
	29	281,0	265,5	257,5	243,5	237,5	220,5	213,5	201,0	197,5	179,5	173,5	161,0	154,5	141,0	133,0	108,0	100,0	86,0	79,5	67,5	60,0	45,5	38,0	29,5	23,0	8,5	1,0	346,0	338,5	326,0	318,5	298,5
	30	288,5	274,0	265,5	251,5	245,0	228,5	221,5	210,0	205,5	187,5	181,0	168,0	161,5	149,5	142,0	115,0	108,5	94,5	87,0	74,0	68,0	54,5	46,0	38,5	31,5	15,5	8,0	355,5	349,0	332,5	326,0	297,5
	31	302,0	287,5	279,0	264,5	258,5	241,5	235,0	223,5	218,5	202,0	195,0	181,5	175,5	164,0	155,0	130,5	123,5	110,0	101,0	89,5	82,5	69,0	60,0	52,5	46,0	29,5	23,5	9,5	3,5	349,0	340,5	320,0
	32	312,5	296,5	289,0	275,0	266,5	249,5	243,0	233,0	229,0	210,0	204,0	190,5	184,0	172,0	164,5	139,0	132,5	118,0	111,0	98,5	92,5	77,5	69,5	61,5	55,0	40,0	32,5	18,5	12,0	358,0	350,5	321,5

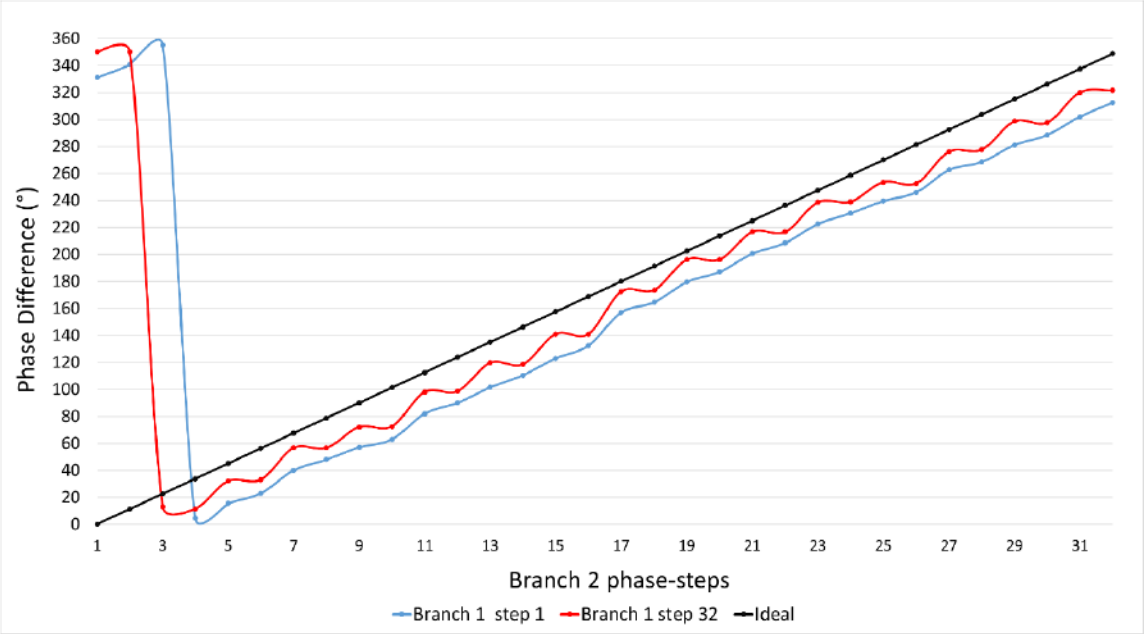

Figure 18. Phase Difference between branch 1 and branch 2.

Table 3 presents the data referring to minimum, maximum, average, and the standard deviation when assuming a normal distribution regarding the phase increment given phase-step change for branch 2. The average phase-shift in branch 2 is illustrated in Figure 20.

Similar to branch 1 phase increment Δ15-16, branch 2 increment Δ16-17 presents a higher, maximum, minimum, and average, and the reason possibly follow an expected behavior presented in the datasheet of the component, TriQuint TGP2100, where at phase-step 17 there is significant change in phase error due to activation of last bit-switch, which might be considered a discontinuity and an effect from the quantization behavior.

The results obtained in the phase-shifter phase-step analysis and their deviations shows how resourceful and important is this test for the characterization of the individual phase distance of each phase-shifter and its phase-steps. A complete characterization would clearly allow the possibility of designing a constrained optimization that could minimize the errors. And therefore, permit the construction of a map of phase-shifters and corresponding phase-steps to achieve the relative phases defined in the expected operation of the beamforming, beam-steering among other phase related technologies in an optimum way.

Next section focus on two objectives, to analyze the possibility of obtaining quicker results through power measurements using the spectrum analyzer and to test the phase drift in the results caused by the operation in a different frequency.

Table 2. Analysis of phase-shifter phase-step increment, branch 1, assuming a normal distribution

Branch 1				
Phase-shifter increment	Minimum Phase Shift (°)	Maximum Phase Shift (°)	Average Phase Shift (°)	Standard Deviation (°)
Δ32-1	-19,0	-6,5	-12,55	4,20
Δ1-2	-16,5	-13,5	-15,13	0,71
Δ2-3	-10,5	-7,0	-8,17	0,69
Δ3-4	-15,5	-12,5	-13,97	0,87
Δ4-5	-9,0	-5,5	-6,88	0,92
Δ5-6	-18,0	-15,0	-16,45	0,93
Δ6-7	-8,5	-4,0	-6,75	0,83
Δ7-8	-13,5	-10,0	-11,28	0,86
Δ8-9	-8,0	-3,5	-5,72	0,97
Δ9-10	-19,0	-15,0	-17,02	0,92
Δ10-11	-8,5	-4,0	-6,52	0,91
Δ11-12	-15,0	-11,0	-12,86	0,98
Δ12-13	-9,5	-5,5	-6,83	0,89
Δ13-14	-14,5	-9,5	-12,22	1,04
Δ14-15	-10,5	-6,5	-8,39	1,00
Δ15-16	-29,5	-23,5	-26,34	1,45
Δ16-17	-9,5	-6,0	-7,08	0,98
Δ17-18	-16,0	-12,5	-13,95	0,89
Δ18-19	-9,0	-5,0	-7,42	0,93
Δ19-20	-14,5	-10,5	-12,64	0,94
Δ20-21	-8,5	-4,5	-6,56	0,92
Δ21-22	-16,5	-12,5	-14,14	0,91
Δ22-23	-10,0	-5,5	-7,69	1,02
Δ23-24	-10,5	-6,0	-8,06	0,93
Δ24-25	-8,0	-4,0	-6,33	1,05
Δ25-26	-18,0	-14,0	-16,06	1,02
Δ26-27	-9,0	-5,5	-7,17	0,89
Δ27-28	-15,0	-11,5	-13,13	0,98
Δ28-29	-9,0	-5,0	-6,81	0,96
Δ29-30	-16,5	-12,5	-14,50	1,02
Δ30-31	-9,5	-6,5	-7,75	0,79
Δ31-32	-31,0	-17,0	-23,64	4,31

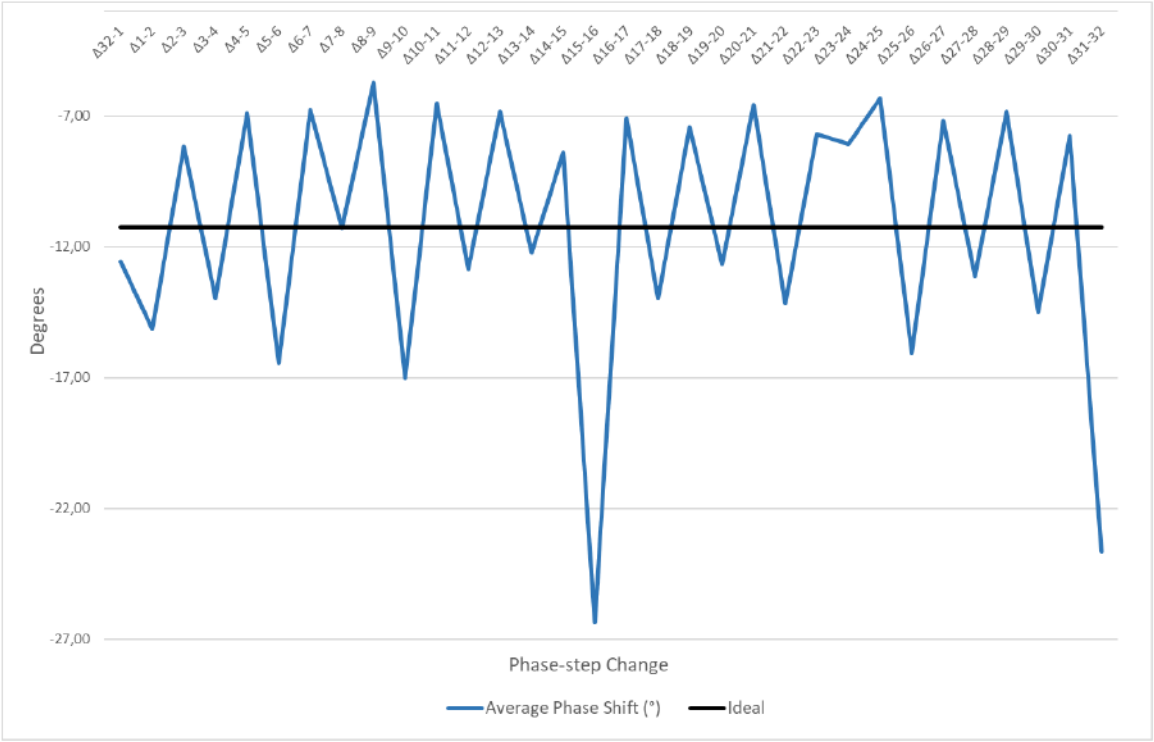

Figure 19. Branch 1 average phase-shift.

Table 3. Analysis of phase-shifter phase-step increment, branch 2, assuming a normal distribution

Branch 2				
Phase-step increment	Minimum Phase Shift (°)	Maximum Phase Shift (°)	Average Phase Shift (°)	Standard Deviation (°)
Δ32-1	18,5	23,5	20,90	1,36
Δ1-2	6,5	10,5	8,50	0,97
Δ2-3	13,0	16,5	14,65	0,86
Δ3-4	7,0	10,0	8,56	0,76
Δ4-5	9,5	14,0	11,82	0,99
Δ5-6	6,0	10,0	7,55	1,04
Δ6-7	14,0	18,0	15,69	1,05
Δ7-8	5,5	9,5	7,71	0,86
Δ8-9	8,0	12,0	9,76	0,93
Δ9-10	4,5	8,5	6,52	0,94
Δ10-11	15,0	19,0	16,97	0,92
Δ11-12	5,5	9,5	7,45	0,96
Δ12-13	10,0	14,5	12,10	0,99
Δ13-14	5,5	10,5	8,27	1,01
Δ14-15	11,5	15,0	13,21	0,79
Δ15-16	8,0	12,0	9,58	1,01
Δ16-17	21,5	24,5	22,71	1,05
Δ17-18	6,0	10,0	8,27	0,97
Δ18-19	12,0	17,0	14,73	1,01
Δ19-20	6,5	10,5	8,61	1,05
Δ20-21	10,5	15,0	12,29	1,09
Δ21-22	6,5	11,5	8,26	1,15
Δ22-23	11,0	16,0	14,56	1,05
Δ23-24	6,5	11,0	8,63	1,10
Δ24-25	6,5	10,0	8,05	0,87
Δ25-26	5,5	9,0	7,08	0,88
Δ26-27	14,5	18,5	16,47	0,87
Δ27-28	6,0	10,0	7,48	1,02
Δ28-29	10,0	14,0	12,32	1,00
Δ29-30	6,5	10,5	8,00	0,90
Δ30-31	13,0	16,5	14,18	0,87
Δ31-32	8,0	10,5	9,11	0,82

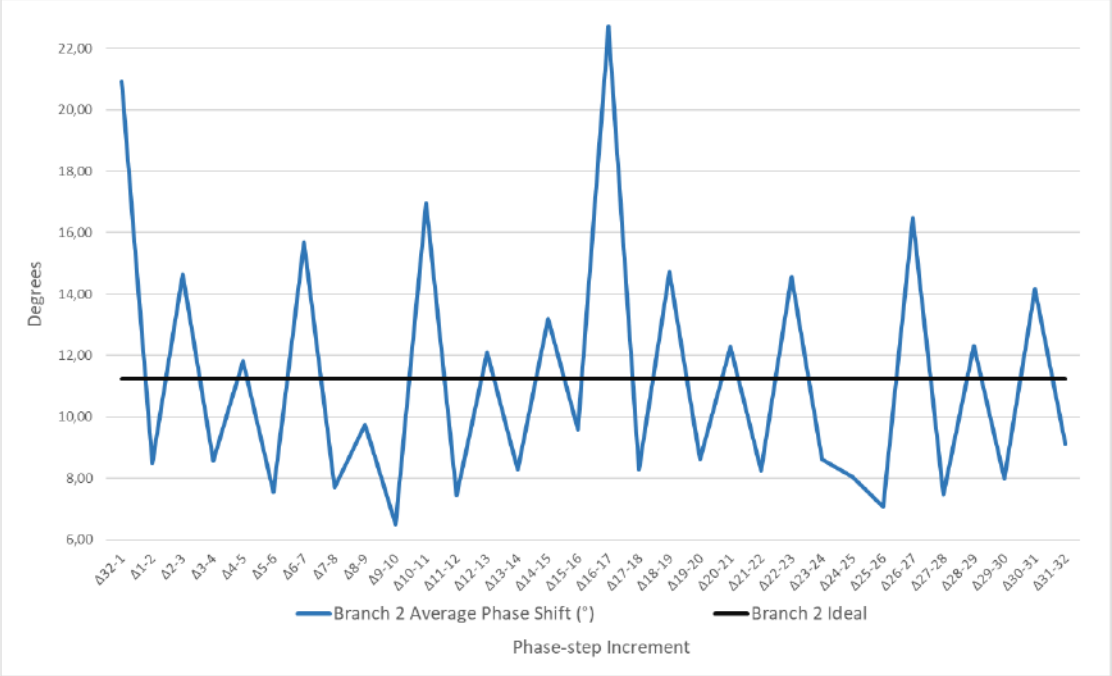

Figure 20. Branch 2 average phase-shift.

5.2. Test 2: Phase Difference Test and Frequency Dependence – Using Power as a Proxy

Test 2 aims to show the trade-off between Test 1 and a test using the variable power as a proxy to obtain the values of phase. The trade-off presented is the exchange between accuracy and longer test times, against a fast but error prone test. The discussion is focused on the phase-shifter component and its behavior, and further exemplified with the phase drift experienced by the system when operating at different frequencies.

Two methods were proposed in Chapter 4.2 to acquire the phase values from the power values. The first method, starts with the global maximum and minimum power (dBm) from a table of branch 1 (reference) and one other branch N (2-8), this allows the construction of a table to compare phases (°) to power levels (mW).

The first method diminishes the amount of work needed to achieve the results, but is dependent of the strong assumption that throughout the component there is no difference in matching, impedance, etc., that would affect the signals, in a way to vary the combination of results, e.g. when both signals, from branches 1 and N combine at the same phase and different phase-shifter phase-step, they would always have to present the same power level. This assumption is not real. When dealing with the studied phase-shifter component, it's clear that the interaction of the signals from the two components don't maintain a singular power level.

Two different sets of data corroborate to discard this method, the Test 1 power levels, i.e. the power levels where branch 1 and 2, at 32 × 32 phase-steps, would reach 0° and 180°. And Test 2, when this method is applied the result would departure from global maximum and minimum. Comparing the values of maximum for a determined step of branch 1 or 2 to all the steps from the other branch, the result would be several degrees apart from reality, causing differences of more than 70° in some cases. The reasons, as already mentioned, might include different properties and characteristics of the different paths inside the phase-shifters.

The second method tries to tackle the problems from method 1. It sets the maximum and minimum power references at the branch 1 phase-step level. Branch 1 is considered the reference, and for each of its phase-shifter phase-steps, and within branch N (1-32) steps, is selected a minimum and maximum power value as reference. Once the values are selected, they are scaled to the mW scale and a table relating phase and power is created from the maximum and minimum power difference.

A last correction is needed due the phase difference between the measurement setup, the cables and the power divider. The setup was measured at the VNA and its S-parameters were recorded and the values referring to the expected frequencies were calculated, and compensation applied following the methods in [16].

For selected frequencies the phase correction needed for the power divider compensation is presented in Table 4.

As already discussed in Chapter 4.2, since this method establishes the reference values, minimum and maximum, as 0° and 180°, it adds errors in all the sets of phase-steps. The added errors will be correlated to the errors made when setting the reference. These errors are the result of a compromise between time and accuracy, derived from using the power as a proxy to establish phase values instead of the VNA tests. The errors tend to be smaller as in the future the tolerances and specifications of the phase-shifter components become stricter.

Table 4. Power divider phase compensation for selected frequencies

Frequency (GHz)	Phase (°)
26	-145,3
27	-136,92
27,5	-132,68
27,9	-129,29
28	-128,53
28,1	-127,70

Test 2 was executed over branches 1 and 2, over the whole set of phase-steps (32×32) and 31 frequency points, 26 to 29 GHz (0,1 GHz), the consumed time was approximately 6 hours and 30 min. The full set across the eight branches is expected to consume 45 hours.

The results of the Test 2 made using the second method and the spectrum analyzer are compared with the phase values presented in the Test 1, with the VNA. The phase deviations from the results of Test 1 are considered a phase-error, the comparison is summarized in Table 5.

The scaling technique and data manipulation used in the second method also appears to distort the result. While the values around 0° and 180° are among the values with the lowest phase-error, the values around 90° and 270° suffer with severe distortion, causing the high phase-errors observed in Table 5.

The average phase-error per phase-step is illustrated in the Figure 21. Branch 1 phase-steps 16 and 32 have distinct higher phase-errors since the scaling did not count with the previous errors encountered in Test 1.

The distortions of the method used during Test 2 also impact on the analysis possibility of the phase-step increment similarly to what was performed in Test 1. The same applies to the analysis of the frequency drift, since the distortions cannot be significantly separated from the drift without a high number of data observations.

The power measurement and scaling performed in Test 2 will still be applied for Test 3 despite its underperformance, due to the scaling method and phase-errors. During the next section the same scaling technique will be applied on the other branches to construct a phase calibration table for the RF transceiver as a power measurement, and as a faster option to the phase difference characterization performed with the VNA.

Table 5. Phase-error, comparison between Test 1 (reference) and Test 2, for branches 1 and 2

	Branch1			Branch2		
Phase-Step	Minimum Phase-Error (°)	Maximum Phase-Error (°)	Avg. Phase-Error per Phase-Step (°)	Minimum Phase-Error (°)	Maximum Phase-Error (°)	Avg. Phase-Error per Phase-Step (°)
1	0,01	29,67	*13,14*	0,53	25,41	10,05
2	0,86	40,81	*15,53*	0,33	24,29	9,41
3	0,20	33,11	*13,99*	0,27	27,84	10,86
4	0,15	35,88	*13,71*	0,10	27,66	11,56
5	0,47	25,03	*12,97*	0,46	25,06	13,33
6	0,11	31,98	*13,76*	0,32	28,47	13,09
7	0,46	29,06	*12,82*	0,57	33,32	14,28
8	0,82	24,65	*12,49*	0,65	37,20	14,60
9	2,86	28,72	*14,35*	0,11	36,61	15,22
10	0,15	27,84	*12,51*	0,05	39,09	15,67
11	0,46	26,49	*12,02*	0,14	36,24	13,65
12	0,63	24,30	*12,38*	0,63	40,81	14,74
13	0,33	26,84	*12,26*	0,82	29,48	13,11
14	0,39	27,77	*12,01*	1,27	35,88	14,64
15	0,27	21,04	*10,93*	0,29	26,67	13,31
16	0,02	39,09	*18,97*	0,01	31,98	13,62
17	0,76	20,61	*10,74*	0,03	28,30	12,60
18	0,02	27,07	*12,32*	1,53	30,11	13,28
19	0,05	23,34	*12,97*	0,39	30,74	13,16
20	0,83	31,97	*14,61*	0,69	29,94	13,87
21	0,63	25,03	*13,94*	1,05	30,23	13,23
22	0,14	31,54	*13,65*	0,53	30,05	13,69
23	0,10	23,83	*12,55*	1,66	29,65	13,20
24	1,64	23,10	*12,00*	0,02	26,64	12,93
25	0,28	25,02	*12,21*	0,83	30,62	13,86
26	1,26	30,74	*13,01*	0,15	32,20	13,54
27	0,04	23,00	*11,60*	2,02	28,58	12,78
28	0,45	29,94	*12,25*	0,97	27,50	13,83
29	1,81	23,66	*12,15*	1,11	27,62	13,79
30	0,51	30,23	*14,58*	1,26	31,97	15,81
31	0,03	23,02	*12,30*	0,15	26,69	12,73
32	2,32	44,06	*22,55*	0,02	31,54	13,76

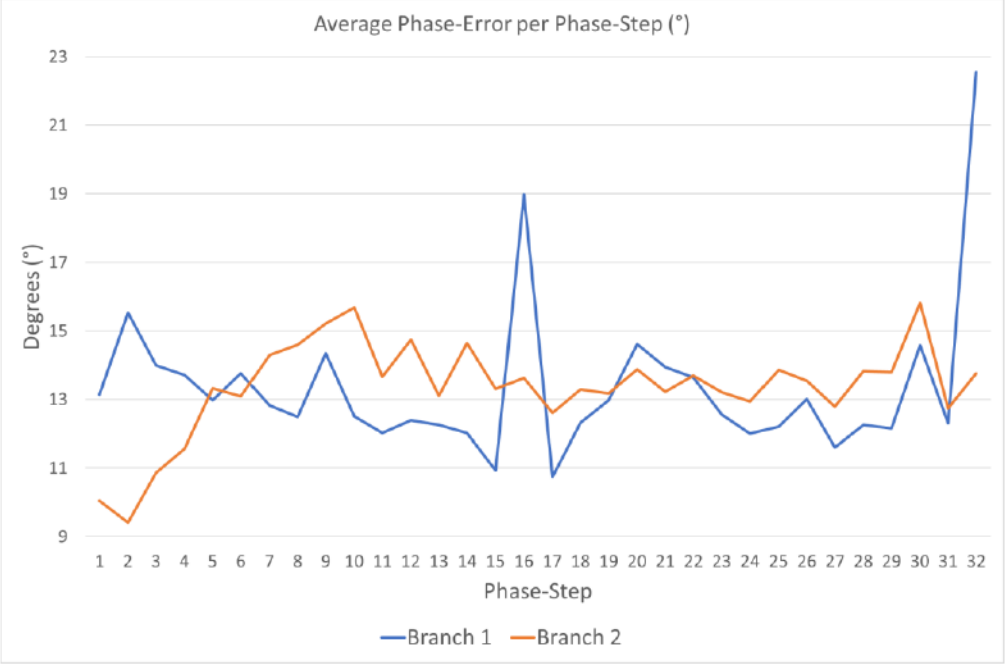

Figure 21. Branches 1 and 2, average phase-error per phase-step.

5.3. Test 3: Phase Difference across the RF Transceiver Branches – Using Power as a Proxy

The main goal of this test is to acquire the data to construct a relative phase table to calibrate the phase-shifters. The phase table can be optimized given the required phase values for a phase related technique e.g. beam-steering.

The same procedure used on the second method presented in Test 2 is applied to all the remaining branches, but to retain the simplicity, the test is performed only at 28 GHz. The test regarding all branches, branch 1 as reference, and measurement from branches 2 to 8 at 28 GHz takes 1 hour and 30 minutes. For all the frequency range 26 to 29 GHz, it would take approximately 45 hours.

The results obtained for branches 3 to 8 have no previous data to be compared against, but all the negative characteristics from Test 2 analysis at the previous section might hold. The scaling technique and data manipulation might distort the results given the departure from the relative phase of 0° and 180° when compared to branch 1.

Once the data was acquired, and intending to obtain a set of relative phases which are the closest possible to the required set of phases an optimization method is required. The objective of the optimization is to minimize the difference between the required set of phases and the relative phases gathered by the Test 3. As an example, a set of phases is required for the branches to perform the beamforming at 0°. A subset of all the possible relative phases regarding phase-steps of branches 2 to 8 was constructed for each phase-step of the reference branch, branch 1, resulting in 32 subsets. One of the subsets is presented in Table 6.

For each subset, a set of phase-steps is selected for each branch, according to the minimization of difference between the required phase and the relative phase in the subset table. A new optimization is then made comparing the results of each subset, and again minimizing the difference between required and relative phases.

Despite the distortion problems, this method benefits from utilizing the whole spectra of possibilities given by the phase-shifters. In the Section 5.5 this method is applied to perform the radiation pattern test, and the set of required phases will be supplied by the requirements of the beamforming and beam-steering techniques.

In the next section a different method derived from Test 1, data gathering from the VNA, will be proposed. And finally compared with the method presented in this section within the radiation pattern test in Section 5.5.

5.4. Test 4: Phase Difference across the RF Transceiver Branches – A variant of Test 1

Test 1 contains information regarding all the data set of phase-shifters phase-steps and is highly accurate, and that causes Test 1 to be particularly cumbersome due to the length of the test.

The amount of information contained in Test 1 allows to determine a compromise in the selection of parameters which could be tested, analyzed and further utilized in the test, and therefore reduce the test duration. The severity of the impact caused by the selection of parameters derivates from the data gathering objective and among other things, the characteristics of the component itself.

Table 6. Relative Phase (°) optimization subset, (1/32), branch 1 – step 1

Branch 1 - Step 1							
	Branches						
Steps	2	3	4	5	6	7	8
1	309,02	312,26	310,15	16,51	349,51	63,98	45,89
2	324,15	308,54	312,56	33,23	357,83	86,32	80,36
3	340,41	328,13	321,93	53,50	18,14	69,81	76,60
4	351,37	332,82	331,33	68,38	29,19	85,71	121,38
5	11,60	347,68	343,85	81,37	51,34	122,86	128,53
6	23,32	356,38	354,50	91,12	61,47	128,30	154,55
7	50,03	40,93	14,16	106,72	84,99	122,52	190,38
8	63,24	62,32	28,14	115,64	95,44	128,53	188,09
9	80,03	72,79	39,30	118,28	111,99	131,19	143,08
10	90,50	83,85	50,57	122,55	118,70	131,69	163,00
11	107,82	100,43	70,96	123,79	121,57	131,11	197,57
12	119,67	119,73	87,62	128,53	128,53	132,16	173,10
13	118,22	100,07	92,47	140,47	138,34	177,70	161,65
14	128,53	114,79	109,71	137,60	133,39	184,45	173,62
15	137,68	121,53	114,07	154,35	153,86	177,76	202,73
16	132,51	128,53	128,53	160,46	154,08	184,56	212,30
17	147,97	315,67	141,61	196,75	179,73	251,53	254,64
18	152,78	310,43	145,46	210,31	186,51	266,33	268,34
19	169,33	331,15	153,58	230,51	209,94	251,79	280,90
20	179,03	334,62	162,96	245,57	218,86	266,42	297,29
21	196,44	349,70	178,73	260,28	238,37	301,41	308,53
22	206,97	353,72	189,98	272,20	247,24	308,53	313,99
23	228,58	41,22	206,68	286,79	269,45	301,46	331,07
24	240,64	60,78	219,95	295,85	277,82	308,54	330,08
25	250,24	72,13	233,65	300,17	287,11	309,65	309,16
26	260,71	83,73	244,93	304,83	293,08	313,35	315,75
27	281,21	101,36	263,81	308,53	305,38	309,59	337,61
28	289,09	119,59	273,76	308,93	307,66	313,36	334,07
29	299,57	104,06	286,77	311,98	308,53	354,27	345,17
30	303,85	115,77	293,98	317,12	310,07	9,53	5,00
31	308,54	122,24	303,72	327,73	317,85	354,22	25,43
32	309,01	128,48	308,52	340,45	323,99	9,73	55,54

The compromise selected for this test refers to the degrees of freedom lying on the analysis of multiple phase-steps at the reference branch, branch 1. Instead of gathering the data from all the phase-steps a smaller subset of at least one phase-step can be measured. The time required for the measurement is drastically reduced when just one phase-step is measured, taking 1 hour and 50 minutes to perform the test. Also, a reduced time for analysis and data manipulation are required, similarly to Test 1 results.

The main positive point of this method is the accuracy of the relative phase values given measurement time, while the main downside is the loss of the possibility of a full optimization along the phase-steps of branch 1. Similarly to Test 3, an optimization technique is used to minimize the error between the required relative phase and the relative phase available at the phase-step table, but differently from Test 3, where all 32 subsets where available, here the choice is made beforehand towards a restrained amount of subsets, leading to a probable second-best solution, or local optimum in the constrained problem.

A second problem arises from the possibility of errors or faults, given the choice for a restrained number of subsets from the phase-step parameter, any fault on the selected phase-step will affect the operation. Two of the possible effects are loss in the output power and distortion of the phase difference. They could occur if one or more of the paths or switches in the component is not working properly.

For the Test 4, branch 1 phase-step 7 was randomly chosen, branches 16 and 32 were excluded as the previous tests showed a strange behavior on those branches. The phase-step table regarding branch 1 phase-step 7 is presented in Table 7.

Table 7. Relative phase (°), phase-step table, branch 1 – step 7

Branch 1 - Phase-step 7							
	Branches						
Steps	2	3	4	5	6	7	8
1	263,5	227,5	248,5	304,0	286,0	341,5	339,0
2	272,0	226,5	260,0	313,5	292,0	352,0	347,0
3	287,0	280,0	273,5	325,5	308,5	343,0	1,5
4	294,5	284,0	283,0	336,0	315,0	352,0	9,0
5	307,0	301,0	294,5	348,5	328,0	27,5	21,5
6	314,5	299,5	304,0	353,5	334,5	39,0	29,0
7	329,5	334,5	316,5	8,0	351,5	27,5	45,0
8	337,5	343,0	325,0	16,5	359,0	37,5	49,5
9	346,5	342,5	334,0	25,0	10,5	68,0	65,0
10	353,0	345,0	341,5	34,0	16,5	76,5	71,0
11	10,5	0,5	357,0	48,5	34,5	68,5	87,0
12	18,0	8,0	4,5	57,0	41,5	79,5	92,0
13	30,0	2,0	15,0	64,5	55,0	108,5	104,5
14	37,5	9,5	24,0	75,5	63,0	116,5	114,0
15	51,0	0,0	35,5	88,5	76,0	109,0	125,5
16	59,5	21,5	45,5	99,5	84,0	117,5	137,5
17	83,5	222,0	71,0	123,5	106,0	163,0	165,0
18	90,5	220,5	82,0	133,5	113,5	173,0	173,5
19	106,0	285,5	94,5	146,0	130,5	164,5	184,0
20	114,5	282,5	103,5	156,0	137,0	172,0	197,5
21	126,0	299,0	113,0	167,0	149,5	204,0	209,0
22	134,0	305,0	121,5	175,5	156,5	215,0	214,5
23	149,0	332,5	134,5	188,0	172,0	206,5	226,5
24	156,0	344,0	144,0	199,0	180,0	217,0	237,5
25	166,0	345,5	150,5	205,0	187,0	246,5	249,5
26	172,5	353,5	159,0	214,5	194,0	254,0	254,0
27	189,5	357,5	171,5	225,0	210,5	246,0	269,0
28	197,0	7,0	178,5	235,5	218,5	253,5	276,0
29	208,0	357,0	189,5	245,5	232,5	287,0	287,0
30	216,5	21,5	197,5	253,5	239,5	298,0	295,0
31	231,5	11,0	209,0	266,5	255,0	287,0	306,0
32	240,0	10,0	220,5	276,0	261,0	297,0	314,0

Given the required phase, determined by the application for the eight branches, the values are normalized against branch 1 step 7 and compared for the branches 2 to 8, minimizing the difference between the required phase and the values available in the table. Finally, a set of phase-steps is chosen to answer the requirement.

Next section compares the results of the methods developed during Sections 5.3 and 5.4 through an OTA test, applying the beamforming and beam-steering techniques.

5.5. Test 5: Over-the-Air demonstration - Applying the phase calibration for Beamforming and Beam-steering techniques

This section aims to demonstrate the performance of the ideas developed in the previous sections, through an OTA test.

The method developed in Test 3, the phase characterization using the measured power level as a proxy to establish the phases, is compared to Test 4, a quick characterization of the relative phases using the VNA with the reference phase-shifter phase-step constrained. Along with them an uncalibrated option is presented, this option refers to the use of the phase-shifter phase-steps as ideal increments, i.e. at each change of the phase-step, the phase relative would change 11,25°. The measurement against the uncalibrated option is a comparison counterpoint to the proposed improvement of the calibration methods.

The setup to perform the OTA test was presented in detail in Section 4.5. Below, in Figure 22, a horn antenna and the RF transceiver mounted on the rotating table inside the anechoic chamber can be seen.

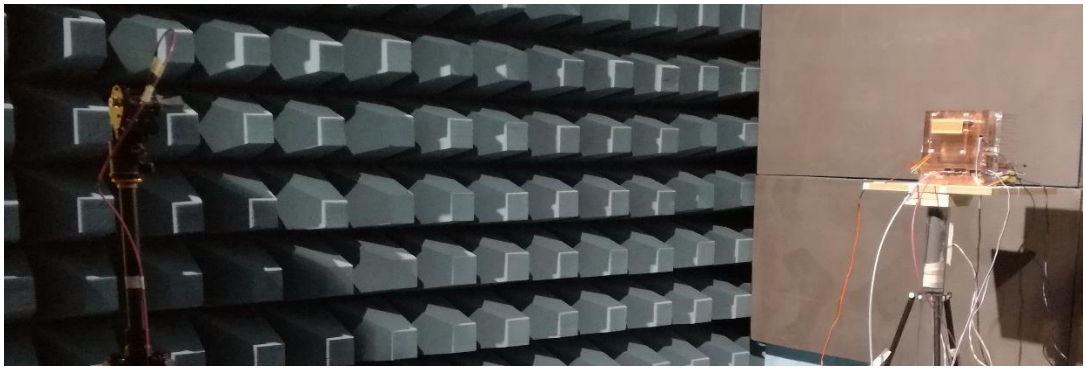

Figure 22. Partial OTA measurement setup, horn antenna and the RF transceiver mounted on the rotating table inside the anechoic chamber.

To apply the beamforming and beam-steering techniques, a direction in which the beam must point is required. This direction is comprised of a set of phases in which the signal must be, relatively to each other, and fed to each element of the antenna array.

The set of phases is determined by the uniformly excited, equally spaced linear array model [13], and generated using the Phased Array System Toolbox in MATLAB. The specifications used are comprised of the spacing between antenna elements, the wavelength referring the frequency used in the test, 28 GHz, and the number of antenna elements.

To simplify, and use a standard procedure, the assumption of uniformly excited elements is made, although this is not the reality of the DUT. The performance of some branches of the DUT are lower than others.

The radiation pattern results are presented with 0° representing a right angle from the face of the planar antenna array, as shown in the Figure 22. A rotation of the table, and consequently the DUT, to the left side has been characterized as a negative increase in the angle, 0 to 90°; and to the right side an increase in the angle, 0 to -90°.

The results presented have been summarized to allow an improved view of the results graphically, and therefore, the presented graphs show different sections of power levels in dBm and different sections of direction angles of the radiation pattern.

Initially, the eight individual branches are measured to demonstrate how they are operating individually at the moment of the test. Figure 23 shows the output power

in dBm for each of the individual branches, from -45 to 45° in the direction angles of the radiation pattern.

Figure 23 shows that branches 7 and 8 receive the signal in an inferior way, and particularly branch 3 can be considered faulty. Such result already impacts the uniform excitation assumption and since this differences in power levels are not accounted for, it will impact on the optimality of the results.

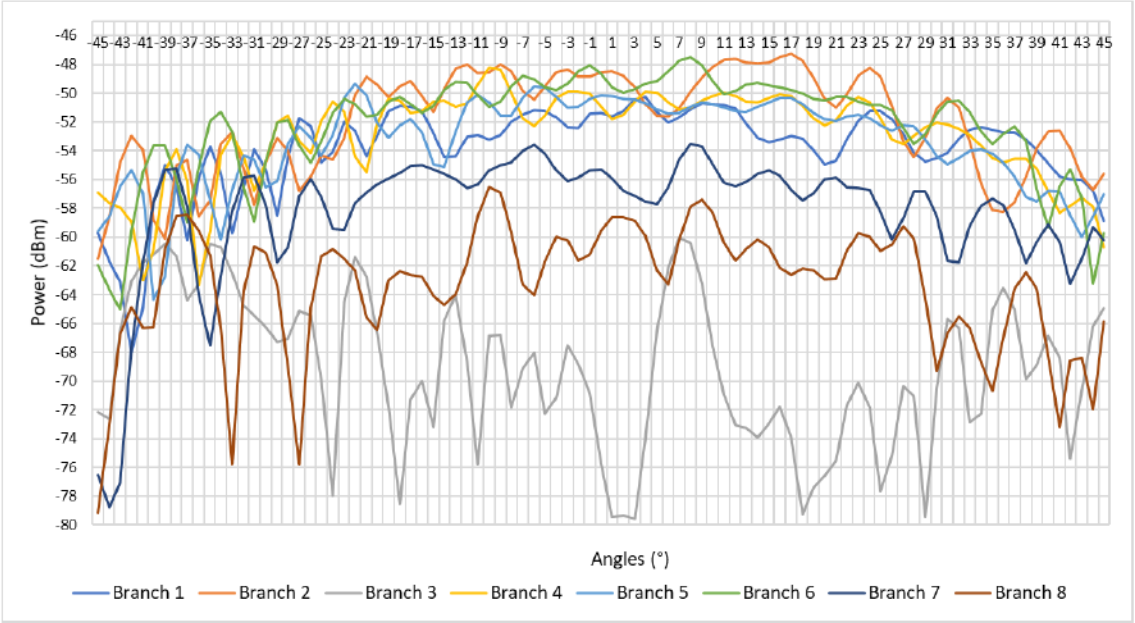

Figure 23. Radiation pattern of the RF transceiver branches activated individually.

The next step is to demonstrate the performance of the beamforming technique in the example case of 0°, receiving the signal perpendicularly to the face of the antenna array. The methods of Test 3, and Test 4 are compared along with the uncalibrated option, and also demonstrate the improvement in the received power due to the antenna array beamforming against the individual antenna element, e.g. branch 4. The results are presented in Figure 24.

The beamforming technique and the use of eight active RF branches improved the gain almost 15 dB due to array gain. At this direction, Test 4 is more accurate than the rest, the right sidelobes are similar to all, while the left sidelobe is 3 dB higher than in Test 3. Despite the non-idealities of the component and the behavior of the phase-step increment analyzed in Test 1, the uncalibrated option presents quite good results, although less accurate and lower in power.

Following, other directions are tested. The results for selected beam-steering angles are presented in Table 8. It includes results regarding: maximum power in dBm, the direction in degrees of the maximum power, the direction error regarding the maximum power when compared to the desired direction, the half-power, or 3 dB beamwidth, which is the angle range in which the power stays within 3 dB from the maximum level; and the Sidelobe Level (SLL) in dB, which is the highest sidelobe power level.

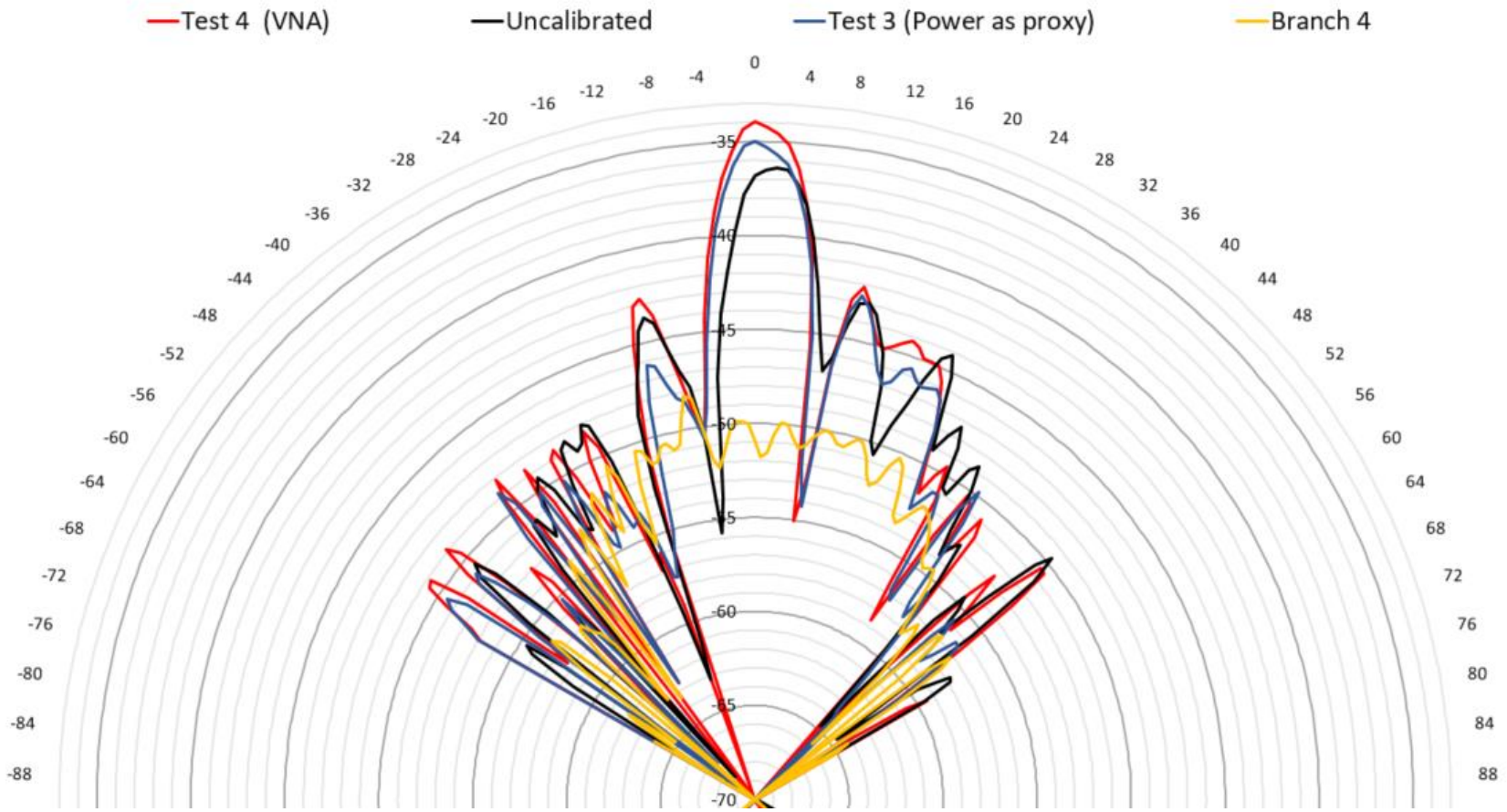

Figure 24. *Beamforming at 0°, radiation pattern (°) vs. power (dBm), comparison of results.*

From the Table 8, a clear accuracy improvement is gained with the calibrations using the methods of Tests 3 and 4.

Table 8. Results for the radiation pattern test, for selected angles

	Radiation Pattern Angle	Max. Power (dBm)	Max. Power (°)	Angle error (°)	Half-power beamwidth (°)	Sidelobe Level (dBm)
Test 3 - Power as Proxy						
	-30°	-37,24	-29	1	7	-42,11
	-20°	-38,49	-18	2	6	-43,73
	-15°	-38,25	-15	0	7	-48,14
	-10°	-33,98	-9	1	5	-41,59
	-5°	-34,23	-4	1	6	-38,23
	0°	-35,02	0	0	7	-43,09
	5°	-35,59	6	1	6	-43,31
	10°	-35,38	11	1	6	-42,17
	15°	-35,72	16	1	6	-44,53
	20°	-38,84	22	2	7	-42,16
	30°	-37,06	31	1	6	-44,83
Test 4 - VNA						
	-30°	-40,06	-28	2	8	-45,38
	-20°	-35,33	-19	1	6	-41,95
	-15°	-36,85	-13	2	7	-44,5
	-10°	-31,06	-9	1	5	-40,58
	-5°	-35,04	-4	1	6	-41,62
	0°	-33,97	0	0	7	-42,13
	5°	-34,38	6	1	6	-43,14
	10°	-35,73	11	1	7	-44,6
	15°	-34,73	16	1	5	-44,24
	20°	-37,91	22	2	7	-43,53
	30°	-38,26	31	1	7	-43,64
Uncalibrated						
	-30°	-39,78	-26	4	7	-43,95
	-20°	-37,46	-18	2	5	-42,61
	-15°	-39,02	-12	3	7	-45,2
	-10°	-37,21	-8	2	6	-44,2
	-5°	-36,08	-2	3	6	-42,62
	0°	-36,38	2	2	6	-42,96
	5°	-34,67	7	2	7	-41,24
	10°	-35,91	11	1	7	-43,99
	15°	-34,77	17	2	5	-41,51
	20°	-36,44	23	3	7	-41,62
	30°	-39,31	32	2	6	-44,57

To illustrate the analysis of the results, Figure 25 presents eight graphs, (a) diverse beam-steering angles for Test 3; (b) diverse beam-steering angles for Test 4; (c) to (h) selected beam-steering direction angles comparing Test 3, 4 and the uncalibrated case.

For Test 3 and 4, in -30° and 30° and beyond there is the occurrence of significant grating lobes, which can be seen in the -30° and 30° directions of Figure 25 (a) for Test 3. The reason for the occurrence lies within the constitution parameters of the antenna array. From Figure 25, the better accuracy of the calibration methods is evident especially for (c) -5°; (e) -10°; and (g) -20°. While at the positive counterparts, the results are similar.

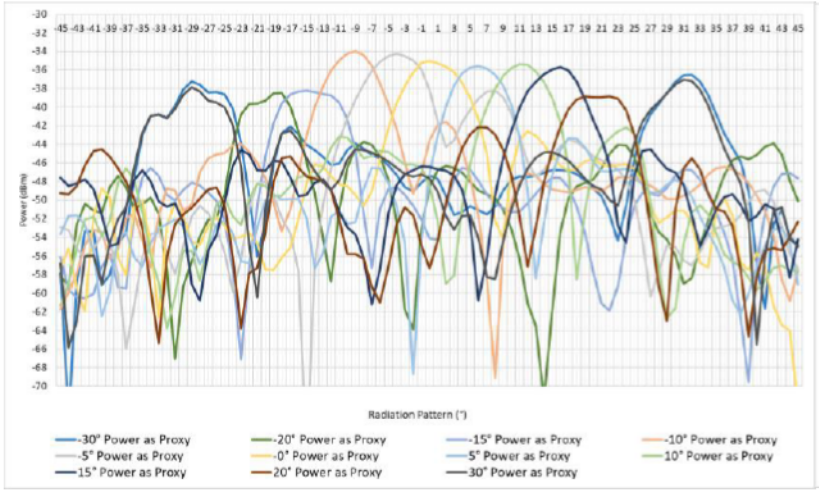

(a) Test 3 – Power as Proxy, for selected angles.

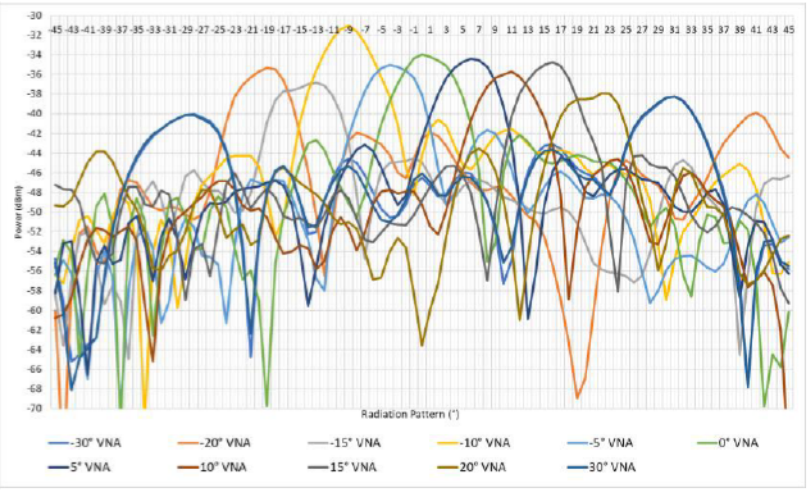

(b) Test 4 – VNA, for selected angles.

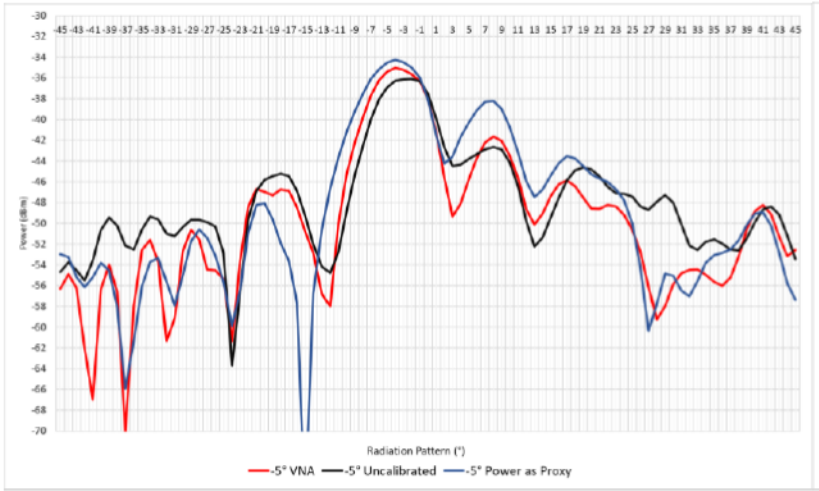

(c) -5°, comparison.

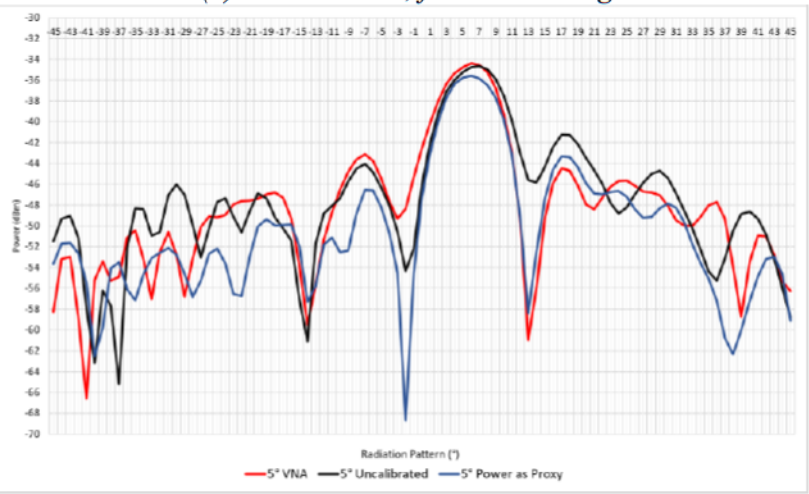

(d) 5°, comparison.

Figure 25. Radiation pattern test, comparisons.

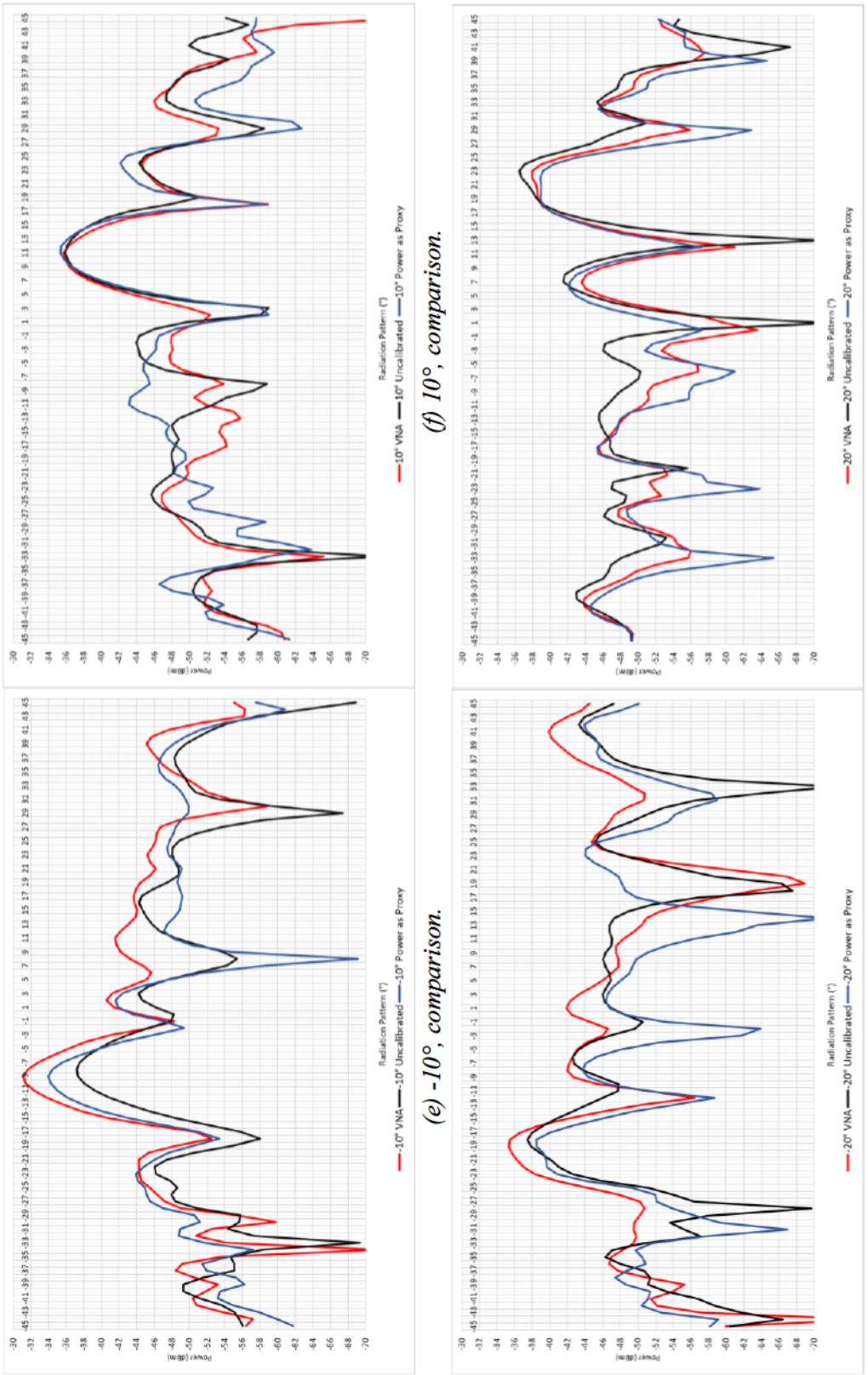

(e) -10°, comparison.

(f) 10°, comparison.

(g) -20°, comparison.

(h) 20°, comparison.

Figure 25. Radiation pattern test, comparisons. (cont.)

The increased sidelobes, the shallow nulls at Test 4 results, and deformities of the beam shape are usually connected with misalignments of the amplitude of the combined signal. In a test facility this occurrence could be traced to the faulty branches. The expected result would resemble that of the Figure 25 (e) for -10°.

The next chapter discusses briefly the tests results comparing the methods presented during the work.

6. DISCUSSION

In order to achieve the end goal of the present work, a brief discussion and a comparison table, Table 9, are presented to summarize the results of different methods used during the work.

Table 9. Comparison between the different methods presented during this work

	Test 1 **Full relative phase characterization**	**Test 2 and 3** **Power as a proxy**	**Test 4** **Partial relative phase characterization**
Time duration for relative phase characterization for one specific frequency	Long	Measurement (Short)/ Data manipulation (Long)	Short
Duration for all branches and one frequency	80 h	1 h 30 min	1 h 50 min
Accuracy of the beamforming	Expected to be higher than Test 4	High	High
Power Gain	Expected to be higher than Test 4	Dependent of scalling model	High
Negative aspects	Long time duration	Performance dependent of the assumptions and the scalling model used. Data manipulation is error prone and has long time duration.	Loss of a degree of freedom from the reference phase-shifter.
Positive aspects	Accuracy/ Fault detection/ Deep analysis of the component behavior	Low time consumption	Low time consumption/Accuracy
Possibility of improvement	Specific setup in the VNA measurement routine could improve the measurement time. Although it would still have a very long time duration.	The scalling model can be improved. The data manipulation can be automatized.	Specific setup in the VNA measurement routine could improve the measurement time.

Tests 2 and 3 where the power is used as a proxy have proven to be the fastest for full characterization of the relative phase without any loss. But the results are dependent on the scaling model used (power-phase) and may present errors due to the same reason. The problem of data manipulation, i.e. scalling, applying corrections for the power divider, etc., can be addressed through automatization, making the problem irrelevant. While Test 1 would only be recommended in the case where the full characterization of the phase regarding a set of components is needed, the main reason is the long time duration of the test.

There is a possibility for improvement in the Tests 1 and 4, regarding the physical setup how the component is attached to the measuring instrument and logical improvements in the test routine.

Overall, Test 4 presented the best results. For one frequency calibration Test 4 is recommended, given accuracy of result, low data manipulation, and short test duration. The main concern of this method rises from the loss of a degree of freedom from the use of only one phase-step of the reference branch, although once errors are expected to be rare, this shouldn't be of major concern.

7. SUMMARY

The present work aims to test and compare different approaches to calibrate the relative phase of an electrically steered phased array.

In the first chapters are presented the definitions regarding the fifth generation of mobile telecommunications, the phased antenna array, the beamforming, and considerations about the new paradigm of communications and signal frequency. Followed by a discussion on test environments, including radiation pattern tests, and errors and issues that might be encountered.

Later, a series of tests are proposed. The aim is to compare two different approaches to measure and obtain the relative phase from a RF transceiver under test. One approach is based on the vector network analyzer instrument, while the other approach focuses on obtaining the relative phase through a proxy, the power level, obtained through the spectrum analyzer.

The system is tested using both approaches against the prediction model, and corrected against deviations due to the uniqueness of the components. The objective was to conform the phase component of a RF phased array transceiver with multiple phase-shifters to be in accordance with specifications of a phased array at low cost and time.

Finally, the results of the proposed approaches were discussed and compared, allowing a recommendation to be made. Possible improvements to the different models are also proposed.

8. REFFERENCES

[1] W. P. 5. ITU-R (2017) Draft New Report ITU-R M.[IMT-2020.TECH PERF REQ] Minimum requirements related to technical performance for IMT-2020 radio interface(s). ITU-R.

[2] Hassett K. (2016) Phased Array Antenna Calibration Measurement Techniques and Methods. In 10th European Conference on Antennas and Propagation (EUCAP), Davos, Switzerland.

[3] Golio M. (2008) RF and microwave circuits, measurements, and modeling. Boca Raton, Florida, USA: CRC Press.

[4] Gorski P., Vigano M. C. and Rio D. L. d. (2017) Developments on Phased Array for Low-Cost, High Frequency Applications. In 11th European Conference on Antennas and Propagation (EUCAP), Paris, France.

[5] U.S. DEPARTMENT OF COMMERCE, National Telecommunications and Information Administration, Office of Spectrum Management (2016) United States Frequency Allocations - The Radio Spectrum. U.S. DEPARTMENT OF COMMERCE, National Telecommunications and Information Administration, Office of Spectrum Management, Washington, DC.

[6] Okumura Y. (2014) 5G Mobile Radio Access System Using SHF/EHF Bands. In Asia-Pacific Microwave Conference, Sendai, 2014.

[7] Suyama S., Okuyama T., Inoue Y. and Kishiyama Y. (2016) 5G Multi-antenna Technology. NTT DOCOMO Technical Journal, vol. 17, no. 4.

[8] Mailloux R. (2005) Phased Array Antenna Handbook. 2nd ed., Norwood, MA: Artech House.

[9] Kim T., Park J., Seol J.-Y., Jeong S., Cho J. and Roh W. (2013) Tens of Gbps Support with mmWave Beamforming Systems for Next Generation Communications. In Globecom 2013 - Wireless Communications Symposium, Atlanta, GA USA.

[10] Veen B. D. V. and Buckley K. M. (1988) Beamforming: A Versatile Approach to Spatial Filtering. IEEE ASSP MAGAZINE, no. April.

[11] Roh W., Seol J.-Y., Park J., Lee B., Lee J., Kim Y., Cho J., Cheun K. and Aryanfar F. (2014) Millimeter-Wave Beamforming as an enabling Technology for 5G Cellular Communications: Theoretical Feasibility and Prototype Results. IEEE Communications Magazine, no. February.

[12] Visser H. (2005) Array and Phased Array Antenna Basics. West Sussex, England: John Wiley & Sons Ltd.

[13] Stutzman W. and Thiele G. (2013) Antenna Theory and Design. 3rd ed., Hoboken, NJ: John Wiley & Sons, Inc.

[14] Dahlman E., Parkvall S. and Skold J. (2016) 4G, LTE-Advanced Pro and The Road to 5G. 3rd ed., London: Elsevier.

[15] Allen B. and Ghavami M. (2005) Adaptive Array Systems. 1st ed., Chichester, West Sussex: John Wiley & Sons Ltd.

[16] Dunsmore J. P. (2012) Handbook of Microwave Component Measurements with Advanced Techniques. Chichester, West Sussex: John Wiley & Sons, Ltd.

[17] Pozar D. M. (2012) Microwave Engineering. 4th ed., Hoboken, NJ: John Wiley & Sons, Inc.

[18] Hansen R. C. (2009) Phased Array Antennas. 2nd ed., Hoboken, New Jersey: John Wiley & Sons, Inc.

[19] Destino G., Kursu O., Tammelin S., Haukipuro J., Sonkki M., Rahkonen T., Pärssinen A., Latva-aho M., Korvala A. and Pettissalo M. (2017) System analysis and design of mmW mobile backhaul transceiver at 28 GHz. In 2017 European Conference on Networks and Communications (EuCNC), Oulu.

[20] 5GCHAMPION (2017) "5G Communication with a Heterogeneous, Agile Mobile network in the Pyeongchang wInter Olympic competitioN. [Online]. Available: http://5g-champion.eu.